Evaluation of 5th Percentile Female ATDs in Near-Side Impact Scenarios Compared to Elderly PMHS

Angela C. Tesny, Clare Fibbi, Yun Seok Kang, Amanda M. Agnew, Gretchen H. Baker,
Yadetsie Zaragoza-Rivera, Benjamin Shurtz, Bengt Pipkorn, Heather Rhule, Kevin Moorhouse,
Craig Markusic, Skye Malcolm, John Bolte IV

Abstract The fatality risk for older crash occupants continues to trend upward with small, elderly females identified as a vulnerable group. During near-side crashes, the thorax remains the most frequent and severely injured body region. The biomechanical responses of 5th percentile female ATDs, the SID-IIs and WorldSID-05F, were compared to the responses of five small, elderly, post-mortem human subjects (PMHS) tested in a realistic near-side crash scenario at 50 kph. Each subject was seated on a mass production seat equipped with side airbag and standard three-point restraint with a pretensioner. One SID-IIs test and four WorldSID-05F tests, two tests using the RibEye multi-point deflection measurement system and two tests using IR-TRACCs, were compared to spinal kinematic corridors created from five PMHS tests and BioRank was calculated using the Biofidelity Ranking System. All five PMHS and each ATD were fitted with a chestband to quantify external chest deflection. Despite similarities in spinal kinematics (BRS<2) and AP chest deflection, differences in lateral chest deflection resulted in inaccuracies in injury prediction from the SID-IIs ATD compared to actual injuries sustained by the PMHS. These results suggest updated injury metrics are needed for current side-impact ATDs to accurately predict injury risk for small females in side-impact scenarios with combined loading present.

Keywords BioRank score, elderly side impact, SID-IIs, thoracic injury risk, WorldSID-05F.

I. INTRODUCTION

Despite a 10% decrease in the total number of fatalities from 2020 to 2021, the number of fatalities for crash occupants over the age of 65 continues to trend upward [1]. Multivariate logistic regression studies using data from the National Automotive Sampling System- Crashworthiness Data System (NASS-CDS) found that females have higher odds of serious injury compared to their male counterparts after accounting for other occupant, vehicle, and crash factors [2-4]. When considering the effect of crash impact type in vehicles with modern occupant protection technologies, near-side crashes have the highest estimated female fatality risk [2]. In the elderly female population specifically, the thorax has been identified as particularly vulnerable [5-8], necessitating further investigation into thoracic injury risk during near-side impacts.

To further investigate thoracic injury in side-impact scenarios, unidirectional lateral thoracic tests using PMHS have been conducted including hub impacts [9-11] and airbag loading [12-13]. Side-impact sled tests have simulated full-body crash interactions, though these studies have mostly looked at mid-sized males or utilised simplified loading conditions that may not be fully representative of the loading conditions created by modern safety technologies [14-17]. Though lateral thoracic deflection is an established injury criterion in side-impacts [14] - [18-19], injury risk has not yet been evaluated in a side-impact scenario where combined loading is present from the anterior-posterior loading due to a seat-belt pretensioner and lateral loading from a side airbag and/or door intrusion, despite occupants being belted in almost every real-world side-impact crash scenario [20].

A Tesny (e-mail: tesny.5@buckeymail.osu.edu, tel: +1 (614)-685-2203) is a Post-Doctoral Scholar and Y. Kang, A. Agnew, G. Baker, Y. Zaragoza-Rivera, and J. Bolte are faculty, staff and students in the Injury Biomechanics Research Center (IBRC) at the Ohio State University in Columbus, OH, USA. B Shurtz is at Autoliv Americas in Auburn Hills, MI, USA. B. Pipkorn is at Autoliv Research in Vargarda, Sweden. H. Rhule and K. Moorhouse are at the National Highway Traffic Safety Administration (NHTSA) in East Liberty, OH, USA. C. Markusic and S. Malcolm are at Honda Development and Manufacturing of America, LLC in Raymond, OH, USA.

Disclaimer -- This paper was funded, in part, under a contract with the National Highway Traffic Safety Administration, an operating administration of the U.S. Department of Transportation, and the opinions, findings and conclusions expressed herein are those of the author(s) and not necessarily those of the U.S. Department of Transportation or the National Highway Traffic Safety Administration. The United States Government assumes no liability for its content or use thereof.

A recent sled test series investigating thoracic response in small, elderly female postmortem human subjects (PMHS) has suggested that this vulnerable group may be experiencing a high number of thoracic injuries due to the combined loading from the seat-belt pretensioner and side airbag [21]. Despite anthropomorphic test devices (ATDs) predicting less than a 15% chance of serious injury, five out of five subjects tested under this combined loading scenario achieved a maximum abbreviated injury score (AIS) ≥ 3. As ATDs have been generally optimised to be unidirectional, results from this PMHS series suggest further investigation is required into the appropriateness of oversimplified PMHS testing to establish injury thresholds and criteria and whether ATDs can accurately capture the kinematics in these more complex crash scenarios. Combined with the evidence that thoracic injuries in the elderly female population are still prevalent despite improvements in vehicle safety, there warrants an investigation into whether current side-impact ATDs are the appropriate safety tools for predicting thoracic injury in a side-impact scenario with combined loading.

In the USA, the Federal Motor Vehicle Safety Standards (FMVSS) [22], the consumer-driven Side Impact New Car Assessment Program (SNCAP) [23], and the side-impact testing conducted by the Insurance Institute for Highway safety (IIHS) [24] all utilise the SID-IIs Build Level D (BLD) as the small female occupant. As a potential advancement and for future crashworthiness assessment, a small female-sized WorldSID (WorldSID-05F) has been developed. Work is still ongoing to define injury risk functions for the WorldSID-05F. As the most appropriate safety tools for evaluating injury risk for small females in a side-impact, these ATDs were selected for further analysis. The objective of this research was to evaluate the capability of the SID-IIs and WorldSID-05F tested in a repeatable, realistic near-side crash scenario to predict kinematic response and chest deflection for small elderly females. Injury prediction capabilities of the SID-IIs were also assessed in this combined loading scenario.

II. METHODS

Test Setup

The biomechanical responses of 5th percentile female ATDs- the SID-IIs and WorldSID-05F- were compared to the responses of five small, elderly PMHS tested in a realistic near-side crash scenario. The vehicle pulse used for this study replicated an FMVSS No. 214 near-side impact to a 2016 compact vehicle with a moving deformable barrier (MDB) at an impact velocity of 50 kph. Data from the Phase I PMHS testing reported in Bolte et al. [21] were compared to the ATD responses in this study. The SID-IIs and WorldSID-05F were subjected to the same realistic near-side impact loading condition as the PMHS, including both the base motion of an impacted vehicle and intruding door, as described in additional detail in Bolte et al. [21]. A summary of the test matrix is found in Table I.

The ATDs were seated in a modern, mass-production driver's seat equipped with a side airbag and a standard three-point belt restraint with a pretensioner which matched the setup of the PMHS tests. The seat was positioned in accordance with the New Car Assessment Program (NCAP) Side Impact Rigid Pole test procedure, apart from the seat being positioned in a mid-track position as opposed to being fully forward [23]. The SID-IIs was seated according to the specifications outlined in the NCAP Side Impact Rigid Pole test. At the time of testing there did not exist a standardised seating procedure for the WorldSID-05F, so the SID-IIs seating procedure was followed. Exemplar seating positions for a PMHS, SID-IIs and WorldSID-05F test are shown in Fig. 1.

The base acceleration of a Hydraulic-controlled, Gas-Energized (HyGE) sled was tuned to match the profile of a vehicle impacted with a delta-V of 50 kph. Door intrusion was replicated using the Advanced Side Impact System (ASIS) (DSD, Linz, Australia) on a HyGE sled (Kitanning, PA). The ASIS contains four independently controlled pneumatic rams that were programmed based on accelerometer data taken from the inner steel structure of a 2016 compact vehicle door impacted by a FMVSS No. 214 MDB [25]. The sled buck and ASIS were instrumented with accelerometers to quantify acceleration of the sled and lateral door intrusion in the Y-direction according to SAE J211 [26].

(a) (b) (c)

Fig. 1. Exemplar seated positions for (a) PMHS (chestband location indicated by dashed red line), (b) SID-IIs and (c) WorldSID-05F.

All subjects, both PMHS and ATDs, were instrumented with axilla level chestbands (Humanetics Innovative Solutions, Plymouth, MI, USA) to quantify thoracic deflection. As the ATDs do not have an axilla landmark, the chestband placement approximated the location to match the measurement location of the PMHS (Fig. 1). Spinal and pelvis instrumentation locations on the ATDs were also targeted to match the locations where data were collected on the PMHS, including T1, T4, T12 and the pelvis at the approximate level of S1. Accelerometers (Endevco 7264C-2K, San Juan Capistano, CA) were installed at these locations on the ATDs to compare to the data reported from the PMHS testing [21] for a direct comparison of acceleration at these locations.

In addition to the chestband installed on the ATDs, thoracic deflection was also quantified using internal ATD instrumentation. Two of the tests run using the WorldSID-05F quantified thoracic deflection using the RibEye multi-point deflection measurement system (Boxboro Systems LLC, Boxborough, MA), an optically based system utilizing three LED lights positioned on the inside of each rib surface. The other two WorldSID-05F tests were equipped with Infra-Red Telescoping Rods for the Assessment of Chest Compression (IR-TRACC). Data were collected from three thoracic ribs for each of the four WorldSID tests. The RibEye data were used to calculate what the IR-TRACC would report, following the methodology outlined in [27], for a direct comparison between measurement methods.

TABLE I
TEST MATRIX

Subject	PMHS	SID-IIs	WorldSID-05F RibEye	WorldSID-05F IR-TRACC
Number of Tests	5	1	2	2
Source of Data	Bolte et al. [21]	Current Study		

Data Analysis

Data were collected at a sampling rate of 20,000 Hz and filtered using a second order, phaseless Butterworth filter in accordance with SAE J211 guidelines [26]. Chestband data were not filtered. High-speed cameras (MotionXtra N3, Integrated Design Tools, Tallahassee, FL) recorded each event at 1,000 frames per second. Chestband processing was completed using CrashStar 2.7 software, then half-lateral, lateral and anterior-posterior (A/P) chest deflection were computed. Half-lateral chest deflection was calculated by determining the point one-half the chest breadth distance from the spine along a vector from the spine to the sternum determined by the pre-impact contour. Lateral deflection was calculated as the change in distance between the two most lateral points on the chestband determined from the pre-impact contour. Additional details regarding chest deflection calculations can be found in Pintar et al. [28].

To quantitatively assess the similarities of the ATD response to the biomechanical corridors created from the PMHS data, Biofidelity Ranking System (BRS) scores were calculated using the most updated method [29]. The BRS score was calculated after aligning the ATD curve in time to the mean PMHS curve. The method of

alignment was signal dependent based on the best approach to align common events [29]. In the context of this study, one of two methods were used: minimum Dummy Cumulative Absolute Difference (DCAD) or zero shift. Further details regarding these methodologies are detailed in Hagedorn et al. [29]. Regardless of which method of phase alignment is used, the Dummy Phase Shift (DPS) is reported as supplemental information, which is the time shift required to align the ATD curve to the mean PMHS curve. To provide context for the DPS, the mean phase shift and maximum phase shift that were required to optimally align the individual PMHS curves to generate the corridor are also reported. As every point included in the BRS calculation will affect the BRS score, only the data that represents the critical response of the event is included in the calculation. This range is determined individually for each signal and is indicated for each calculation. A BRS score greater than 2 indicates an ATD response that is greater than 2 standard deviations from the mean PMHS response curve and a score less than 2 indicates good biofidelity. BRS scores for the lateral, A/P, and resultant accelerations of T1, T4, T12, and the pelvis were calculated as well as for the half-lateral chest deflection measured from the axilla level chestband.

Injury risk prediction capabilities of the SID-IIs in this combined loading scenario were evaluated using previously developed risk curves [18]. The probability of AIS3+ injuries was assessed using maximum rib deflection and peak T12 acceleration using Equations 1 and 2, respectively.

$$p(AIS3+) = \frac{1}{1+e^{(5.8627-0.15498*max.rib\ defl)}} \quad (1)$$

$$p(AIS3+) = \frac{1}{1+e^{(10.5127-0.13*\boldsymbol{age}-0.0536*\mathbf{T12Accel})}} \quad (2)$$

The injury prediction was also assessed using both methods for the PMHS, then compared back to the injury findings from the five PMHS tests.

III. RESULTS

Test input

The vehicle pulse used for this study replicated an FMVSS No. 214 near-side impact to a 2016 compact vehicle by a MDB at an impact velocity of 50 kph. Both the HyGE sled accelerations and velocities across the five PMHS tests and five ATD tests were similar (Fig. 2). The results of the four independent ASIS cylinders, including acceleration, velocity, intrusion velocity, and intrusion distance, for the five PMHS compared to the five ATD tests can be found in the Appendix (Figs A1 to A4).

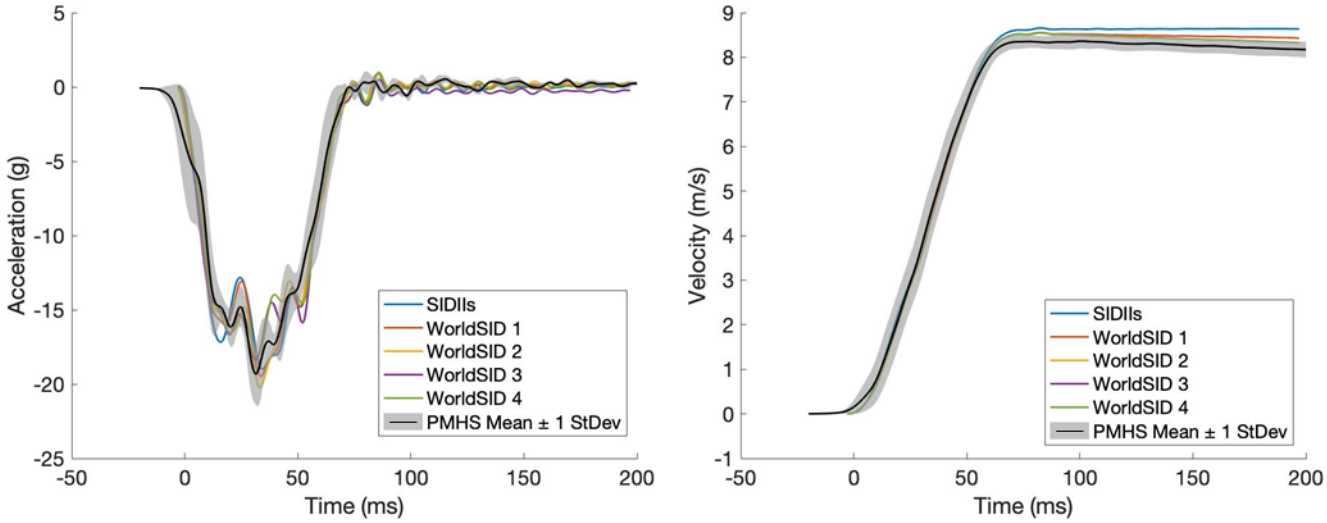

Fig. 2. Sled accelerations (left) and velocities (right) for all ATD and PMHS tests.

Kinematic comparisons

The unshifted response of the ATDs compared to the phase optimised mean curve and one standard deviation corridor of the PMHS data for the resultant accelerations of T1, T4, T12, and the pelvis are shown in Fig. 3. Lateral and A/P acceleration time history plots for each location are found in the Appendix (Figs A5 and A6).

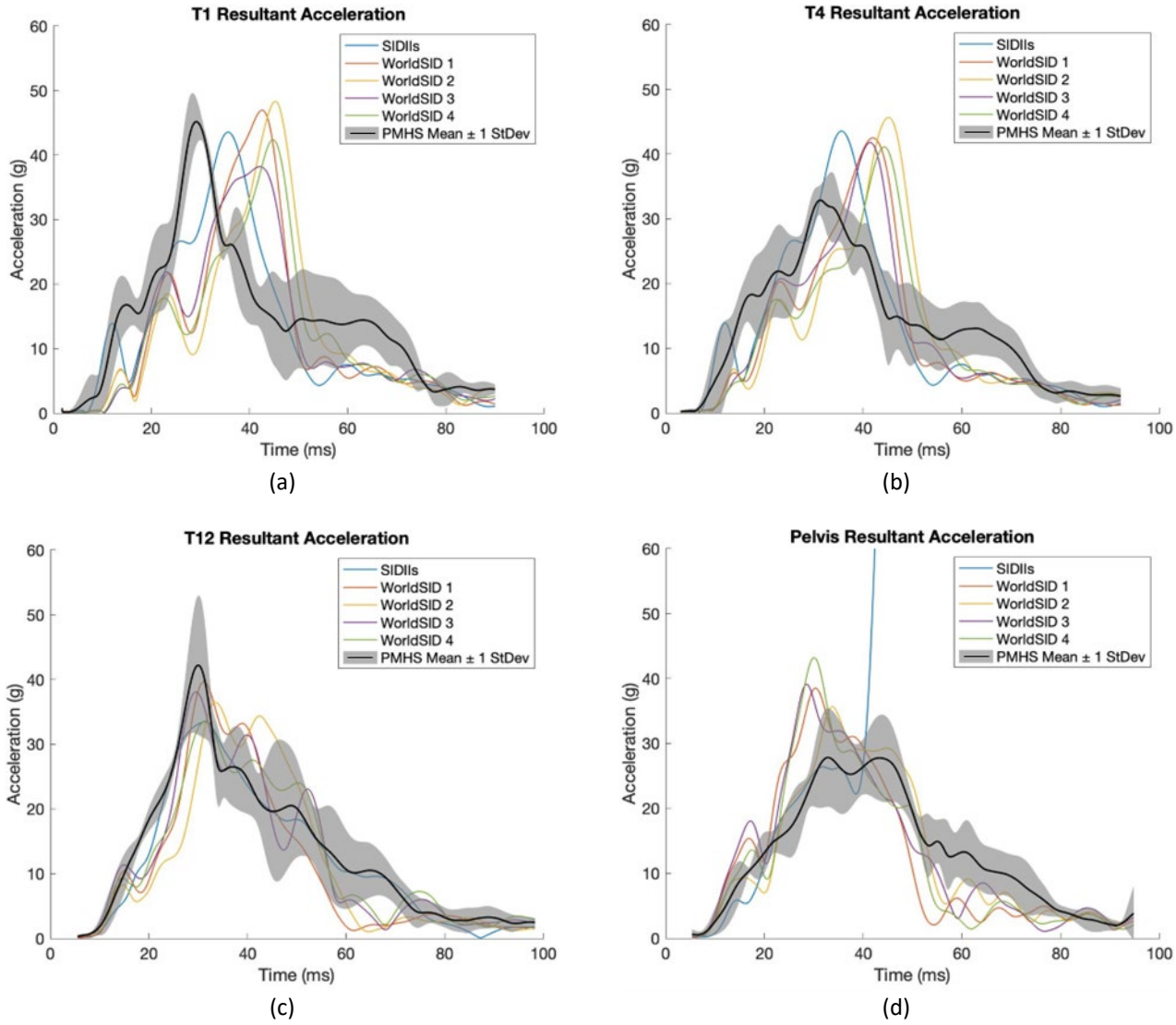

Fig. 3. Unshifted ATD comparison to phase optimised PMHS response corridors of resultant acceleration for (a) T1, (b) T4, (c) T12 and (d) pelvis.

The peak resultant acceleration of all five of the ATD tests occurred after the average resultant acceleration peak of the PMHS in the case of T1 and T4 acceleration, but before the PMHS peak response in the case of the pelvis (Fig. 3). The accelerometer measuring in the y-direction in the pelvis for the SID-IIs test broke during the test, indicated around 40 ms in Fig. 3(d).

Exemplar plots showing the BRS score, DPS, and PMHS phase shift information for the T12 resultant accelerations are found in Fig. 4. The method of ATD phase alignment is indicated in the legend and the range of the BRS calculation is indicated by the dashed blue lines.

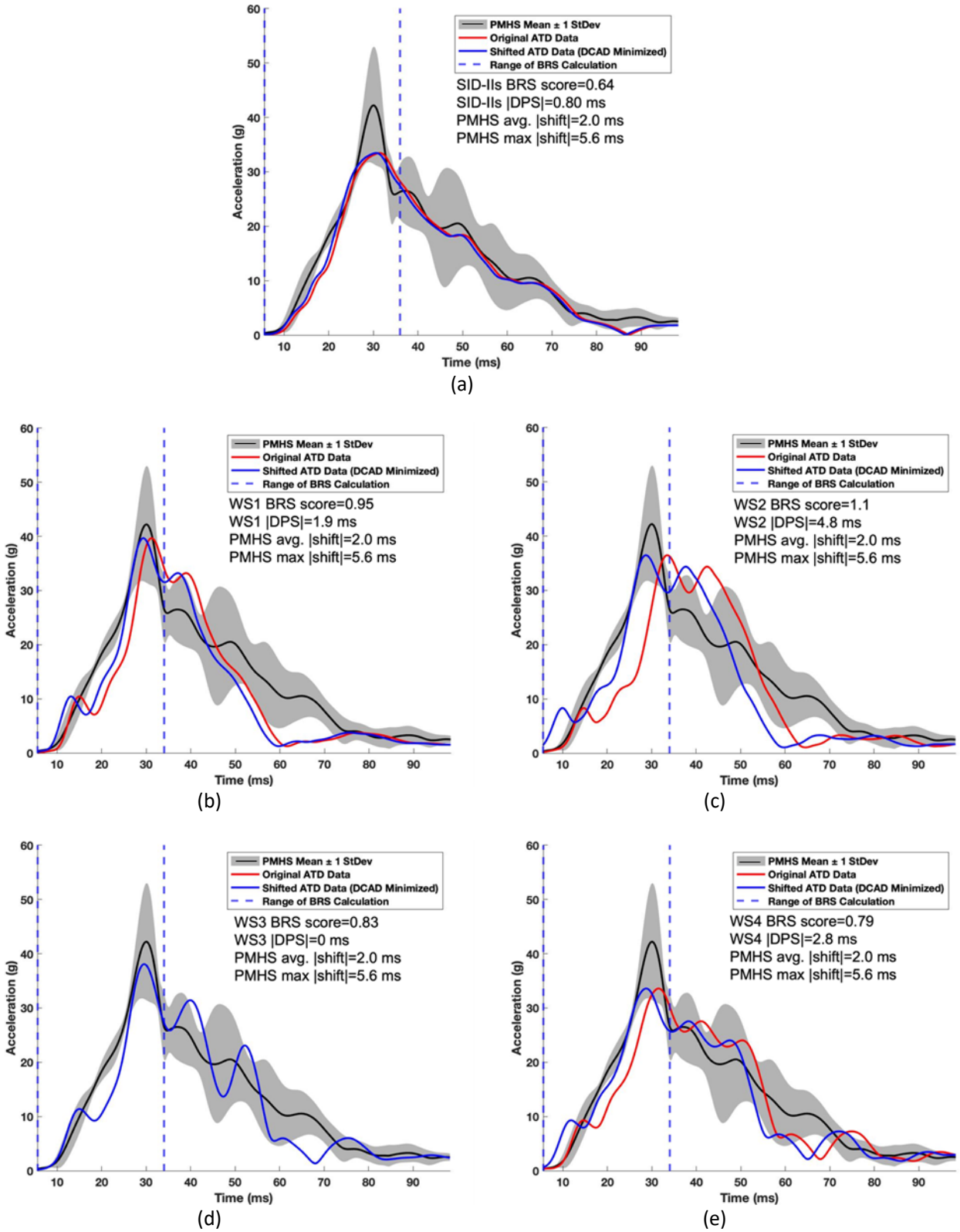

Fig. 4. Exemplar T12 resultant acceleration ATD BRS scores with DPS for the (a) SID-IIs, (b) WorldSID test 1, (c) WorldSID test 2, (d) WorldSID test 3 and (e) WorldSID test 4.

When the DPS is 0 ms, there is no shifting of the data. In this case, the original ATD data and shifted ATD overlap such that the original ATD data are not visible which is exemplified in Fig. 4(d).

The remaining plots are found in the Appendix, Tables A-I to A-IV, which contain the BRS score, phase alignment method, DPS, and PMHS phase shift information in the legend. A summary of the average BRS scores from each ATD test are given in Table II. The table is color-coded to indicate the general degree of biofidelity, where green indicates a BRS score ≤ 1, yellow indicates $1 < \text{BRS} \leq 2$, and red a BRS score >2.

TABLE II
COMPARISON OF BIORANK SCORES CALCULATED FROM T1, T4, T12, AND PELVIS

	SID-IIs	WorldSID Average
T1 A/P	1.4	1.4
T1 Lateral	1.7	2.1
T1 Resultant	1.1	1.4
T4 A/P	1.3	1.1
T4 Lateral	1.1	1.4
T4 Resultant	1.2	1.0
T12 A/P	0.67	0.88
T12 Lateral	0.91	1.2
T12 Resultant	0.64	0.92
Pelvis A/P	0.39	0.85
Pelvis Lateral	0.99	0.94
Pelvis Resultant	0.96	0.9
Average BRS Score	**1.0**	**1.2**

Both the SID-IIs and WorldSID-05F ATDs demonstrated good biofidelity with BRS scores <2, except for the WorldSID average T1 lateral BRS score which was >2. The SID-IIs ATD showed slightly better BRS scores on average compared to the WorldSID-05F ATD. In general, for all ATD tests, there was better biofidelity in the lower spine (T12 and S1) compared to the upper spine (T1 and T4).

Chest deflection

All PMHS and ATDs were fitted with chestbands for direct comparison of externally measured chest deflection. Peak deflections and timing from the axilla level chestband are summarised in Table III and chestband contours at peak deflection are found in Figs A7 to A11.

TABLE III
COMPARISON OF PEAK CHEST DEFLECTION MEASURED BY AXILLA LEVEL CHESTBAND

	PMHS Average ± StDev*		SID-IIs		WorldSID Average	
	Peak (mm)	Time (ms)	**Peak (mm)**	Time (ms)	**Peak (mm)**	Time (ms)
Half-Lateral	**22.2±6.60**	42.8±3.05	**24.9**	35.9	**15.1**	30.7
A/P	**15.4±0.62**	21.1±0.94	**13.7**	12.0	**14.6**	15.6

*Results from Bolte et al. [21]

In general, the ATDs demonstrated peak half-lateral deflection earlier in the event compared to the PMHS. Peak half-lateral deflection measured by the SID-IIs was comparable to the average PMHS response. Conversely, the WorldSID tests showed lower peak half-lateral deflections compared to the PMHS. Plots showing the BRS score and DPS for half-lateral chest deflection measured from the axilla level chestbands are found in Fig. 5.

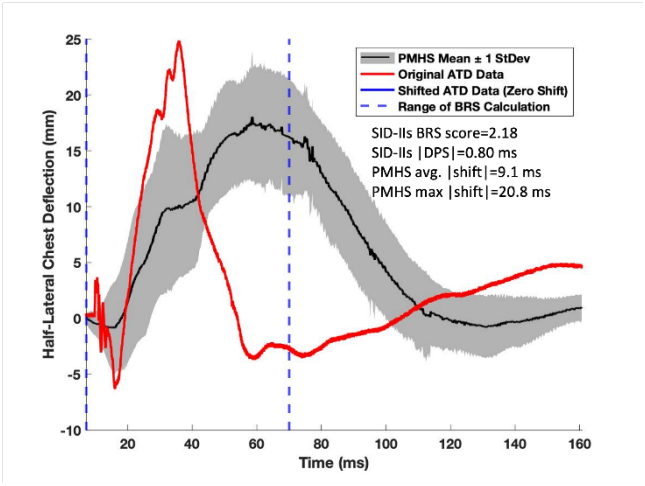

(a)

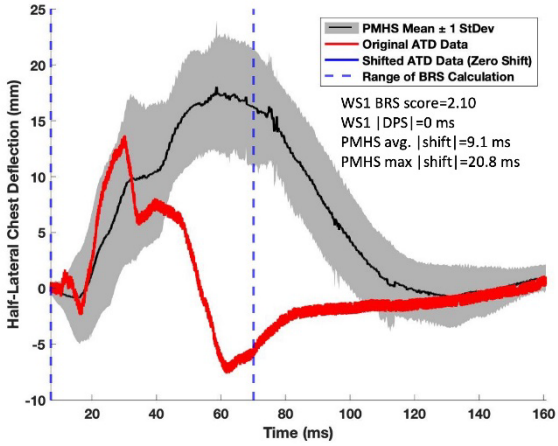

(b)

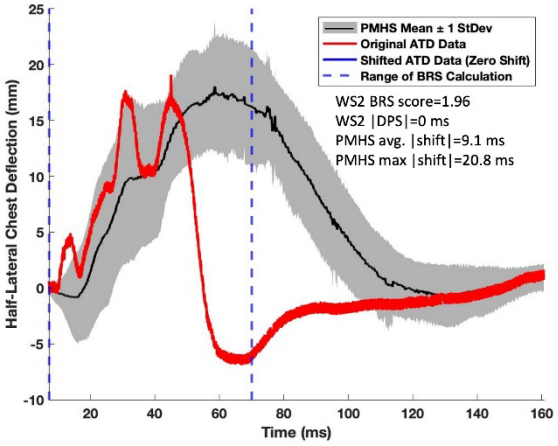

(c)

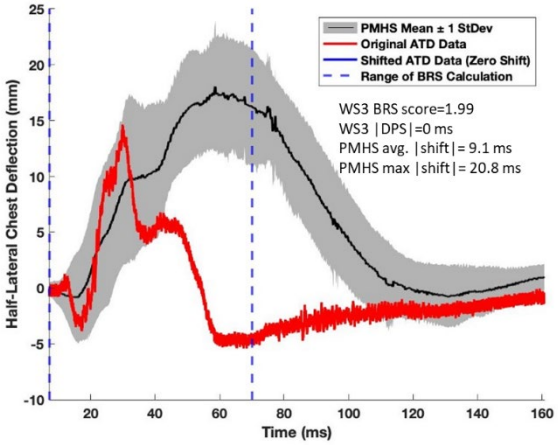

(d)

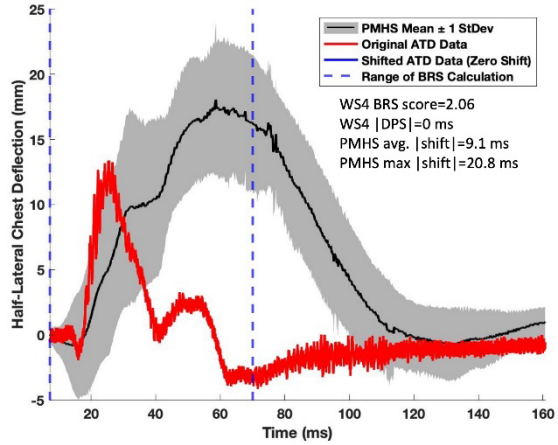

(e)

Fig.5. ATD BRS scores with DPS for the (a) SID-IIs, (b) WorldSID test 1, (c) WorldSID test 2, (d) WorldSID test 3 and (e) WorldSID test 4.

The time history plots comparing the average PMHS chest deflections to the ATD response show a clear difference in thoracic stiffness. The SID-IIs showed a higher peak deflection than the average PMHS response, while the WorldSID tests showed lower peak deflections.

Internal chest deflection measurements from the ATDs are summarised in Table IV. The SID-IIs recorded the highest peak deflection of any ATD test, 26.5 mm from thoracic rib 1. Displacements from all the SID-IIs thoracic ribs were similar to each other.

TABLE IV
COMPARISON OF PEAK CHEST DEFLECTION MEASURED BY INTERNAL ATD INSTRUMENTATION

	SIDIIs		WorldSID 1 RibEye		WorldSID 2 RibEye		WorldSID 3 IR-TRACC		WorldSID 4 IR-TRACC	
	Peak (mm)	Time (ms)	**Peak (mm)**	Time at max (ms)	**Peak (mm)**	Time at max (ms)	**Peak (mm)**	Time (ms)	**Peak (mm)**	Time (ms)
Thoracic Rib 1	**26.5**	35.7	R: 6.53 M: 11.0 F: 13.2 **Max: 13.2**	35.1	R: 6.39 M: 10.6 F: 13.3 **Max: 13.3**	35.6	**15.6**	36.0	**13.0**	39.9
Thoracic Rib 2	**26.0**	34.8	R: 9.93 M: 15.3 F: 15.5 **Max: 15.5**	35.8	R: 8.36 M: 13.6 F: 14.2 **Max: 14.2**	38.8	**17.6**	35.2	**12.0**	37.5
Thoracic Rib 3	**25.8**	34.1	R: 11.7 M: 15.0 F: 16.4 **Max: 16.4**	37.3	R: 11.2 M: 14.5 F: 15.8 **Max: 15.8**	38.9	**12.2**	36.1	**10.2**	37.9

R=rear, M=mid, F=forward measurement locations of RibEye system

Additionally, for each ATD the chestband results were compared to the internal chest deflection measurements at the location that most closely matched the location where the chestband was mounted, the first thoracic rib (Fig. 6).

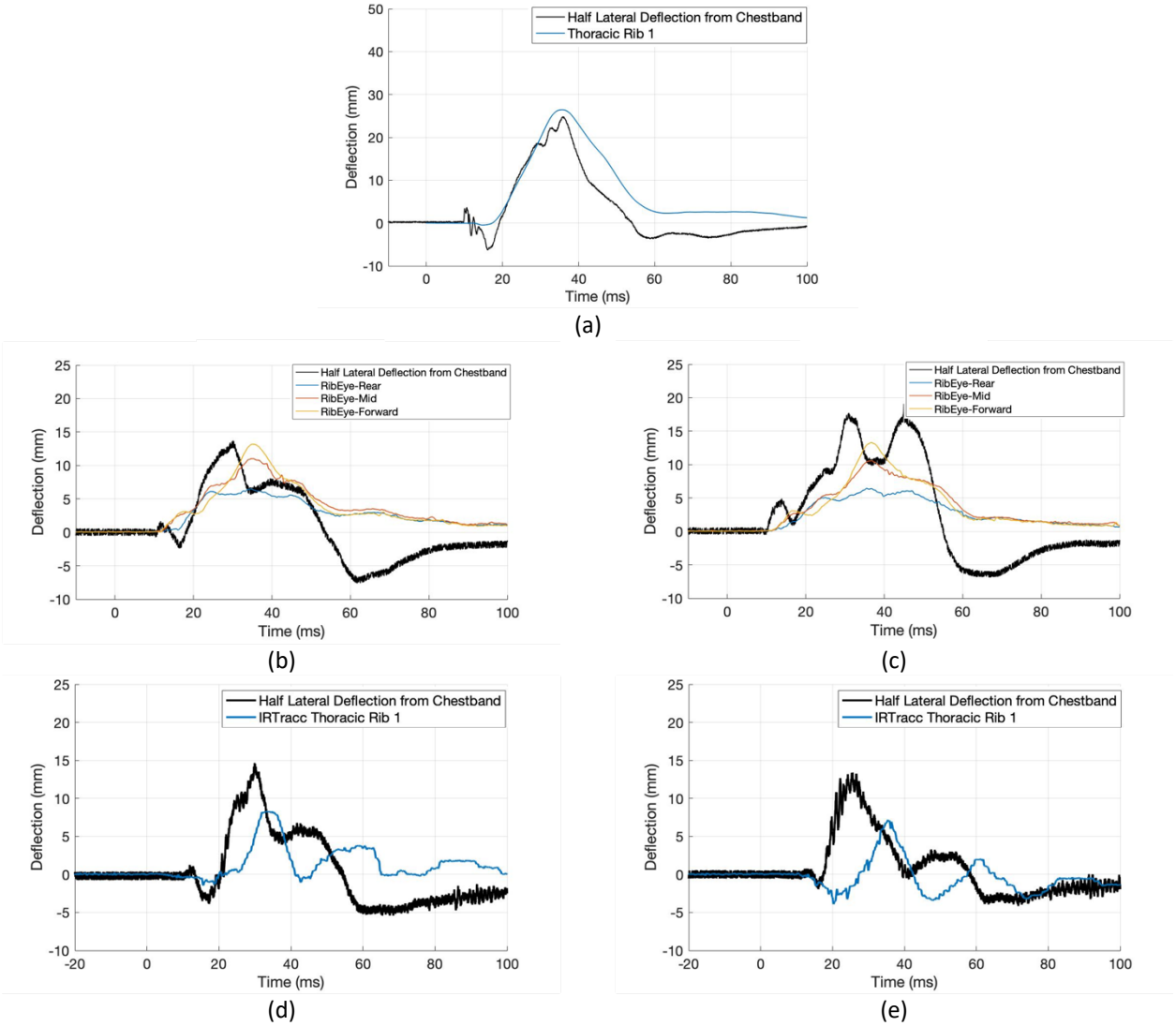

Fig. 6: Chestband deflection time histories compared to ATD internal deflection measurements for the (a) SID-IIs, (b) WorldSID test 1, (c) WorldSID test 2, (d) WorldSID test 3 and (e) WorldSID test 4.

ATD injury prediction

The SID-IIs recorded a maximum peak internal chest deflection measurement of 26.5 mm, corresponding to a 15.2% chance of an AIS3+ injury [18]. In comparison, the average PMHS peak external chest half-lateral deflection measurement was 22.2 mm, corresponding to only an 8.1% chance of an AIS3+ injury (Fig. 7). The injury prediction capabilities of the WorldSID-05F were not evaluated.

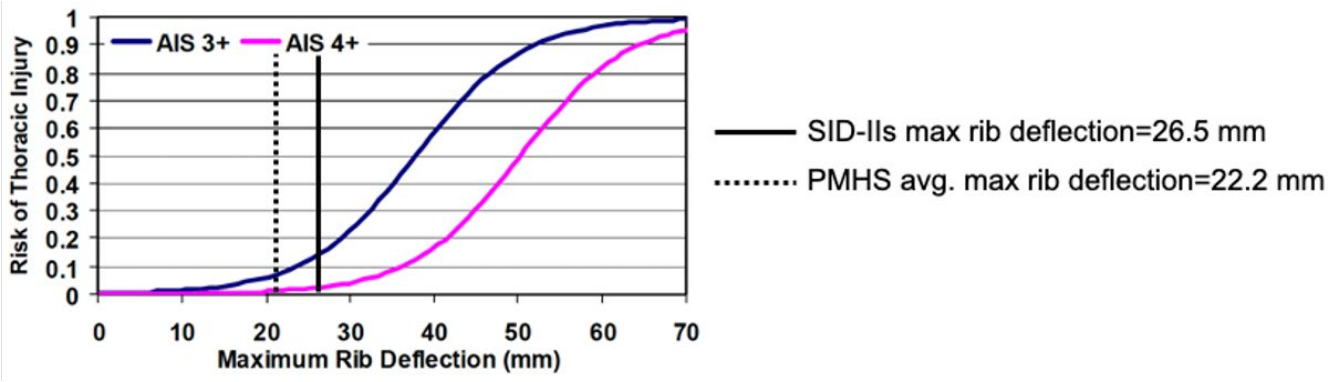

Fig. 7. SID-IIs and average PMHS risk of thoracic injury based on maximum rib deflection [18].

Injury risk prediction was also evaluated using lower spine acceleration (Equation 2) [18]. The risk of thoracic injury based on both rib deflection measurements and peak acceleration of T12 is summarised for the SID-IIs and each of the five PMHS in Table V.

TABLE V
COMPARISON OF THORACIC INJURY RISK BY PEAK RIB DEFLECTION AND PEAK T12 ACCELERATION METHODS ACCORDING TO KUPPA ET AL. [18]

Subject	Age (years)	Peak T12 Acceleration (g)	p(AIS3+) from T12 acceleration	Peak half-lateral rib deflection (mm)	p(AIS3+) from peak rib deflection	Actual AIS score
SID-IIs	***56***	***33.6***	***19%***	***27***	***15%***	***N/A***
PMHS 1	61	36.8	35%	23	9%	3
PMHS 2	83	57.4	97%	31	26%	3
PMHS 3	81	47.6	93%	12	2%	3
PMHS 4	67	41.6	61%	21	7%	3
PMHS 5	69	32.3	55%	24	11%	3
Avg. PMHS	***72***	***43.1***	***68%***	***22***	***9%***	***3***

The SID-IIs predicted only a 19% and 15% chance of thoracic injury from the lower spine acceleration and peak rib deflection methods, respectively, yet all five PMHS sustained AIS3 injuries. Lower spinal acceleration was a better predictor of AIS3 injuries compared to half-lateral rib deflection.

IV. DISCUSSION

The objective of this work was to evaluate the capability of the SID-IIs and WorldSID-05F, tested in a repeatable, realistic near-side crash scenario, to predict kinematic and chest deflection response for small, elderly females. The boundary conditions for the ATD tests were targeted to match the boundary conditions described in detail in Bolte et al. [21]. Both PMHS and side-impact ATDs experienced combined loading of the thorax from loading from the pretensioner and side airbag deployment with realistic door intrusion controlled by the ASIS.

To achieve this objective, five ATD tests were run using the same methodology that PMHS were tested in previously (Table I) for a direct comparison of results. Five experimental PMHS tests were used to capture human variation within the defined population and to define response corridors. Only one SID-IIs test was chosen for further analysis included in this study due to the availability of tests with data that could be directly compared with the PMHS and WorldSID tests. As the SID-IIs is fully defined in Part 572 Subpart V as a proven

repeatable ATD under side impact loading conditions [30], it was determined that a single test could be used for comparison. The WorldSID-05F has not yet been incorporated into Part 572 and is still being evaluated, so each condition (RibEye and IR-TRACC) was run twice.

Comparison of Spinal Kinematics

Although developed primarily from experimental data collected from unidirectional loading, both the SID-IIs and WorldSID-05F demonstrated good biofidelity (average BRS scores <2) of spinal kinematics (Table II). The ability of both these ATDs to properly represent occupant response under these unique boundary conditions indicates the appropriateness of these ATDs in evaluating kinematic response during combined loading scenarios. Generally, biofidelity was better in the lower spine (T12 and S1) for both the SID-IIs and WorldSID compared to the upper spine (T1 and T4), where the peak resultant acceleration of the ATDs occurred later in the event compared to the mean PMHS response, indicating differences in thoracic response between the ATDs and PMHS. These differences may have contributed to the differences seen in measurements of thoracic deflection quantified by the chestbands (Table III). The pelvis is secured to the seat by the lap belt, thus repeatable test inputs resulted in similarities in kinematic response between the ATDs and PMHS in the lower spine. Repeatability in door intrusion controlled by the ASIS resulted in similar loading to the upper spine of the PMHS and ATDs (Fig. A4). This suggests that the differences in thoracic response between the PMHS and ATDs may be attributed to differences in thoracic stiffness and how forces are transmitted from the spine to the individual ribs.

Comparison of Thoracic Deflection

Due to the rib construction in the ATDs, it would be expected to only see deflection on the struck side of the chestband. In the case of the SID-IIs, there is also evidence of deflection on the non-struck side which is visualised in the chestband contour (Fig. A7). If the spine does not adequately transmit loading to the thorax, subsequently causing a global translation of the thorax, this results in reduced loading to the individual ribs which may lead to an underprediction of thoracic injury risk (Table V). The internal thoracic deflection measurement of the SID-IIs demonstrated lower peak deflection compared to the average PMHS response, which is consistent with findings from previous studies that have evaluated thoracic deflection of the SID-IIs in purely lateral or oblique loading [31-33]. However, half-lateral peak deflections measured from the axilla level chestband were similar between the PMHS and the SID-IIs (Table III) despite a clear difference in thoracic stiffness (Fig. 5(a)). The phase optimisation of the PMHS half-lateral chest deflection measured by the axilla level chestband resulted in a maximum shift of 20.8 ms. For the BRS calculation comparing half-lateral chest deflection, the ATD data were not shifted (DPS=0) as the event of interest was the initial loading of the thorax. The time histories of the ATD half-lateral chest deflections show that the ATDs reach peak half-lateral deflection earlier than the PMHS, and the thorax unloads more quickly compared to the PMHS, indicating the thorax of the ATDs is much stiffer compared to the PMHS. The BRS scores for both ATDs were greater than 2 (SID-IIs: 2.18; Average WorldSID: 2.03)

Comparison of Thoracic Deflection Measurement Techniques

When comparing the internal and external measurements of chest deflection for each ATD, the chestband recorded higher deflection measurements than the internal ATD measurements in all cases except for the SID-IIs (Fig. 6). Thoracic rib 1 for the SID-IIs most closely approximates the external chest deflection measurement from the chestband, while the WorldSID ribs respond later and with less deflection. Chestbands have been noted to have a “bulging effect” when used on PMHS because the relatively stiff chestband deflects as an oval without maintaining the true contour of the PMHS under loading. This can lead to overestimations of peak deflections in the A/P direction [10][31], but the accuracy of chestbands used on ATDs has not been fully investigated. The unexpected double-peak contour of the chestband on the second WorldSID test (Fig 5(c)) and variance in A/P and half-lateral deflection results between the four WorldSID tests (Table III) support the notion that the accuracy of using chestbands on ATDs should be further explored before drawing broader conclusions between the internal and external thoracic deflection measurements of the ATDs.

Injury Risk Analysis

A second objective of this work was to evaluate the injury prediction capabilities of the SID-IIs in a realistic side-impact scenario where combined loading occurs. Injury risk analysis for side impacts can be evaluated

using both IIHS and NHTSA criteria. The IIHS evaluates occupant protection in simplified side impacts with a moving deformable barrier with the SID-IIs BLD in the front and rear rows [24]. According to IIHS, for the deflection of each of the three thoracic ribs, a score of "good" is given if all rib deflections are <50 mm and the average of peak rib deflections is <28 mm, which was the case in this study, even though the boundary conditions were different from the IIHS test [34]. Although the SID-IIs fairly accurately replicated the kinematics of the small, female PMHS that were tested (BRS score = 1.03), the ATD severely underpredicted the probability of AIS3 injury. Of note, the data used directly from the PMHS tests similarly underpredicted the probability of AIS3 injury, pointing towards a need to further investigate chest deflection as an injury metric in this combined loading scenario. The SID-IIs thoracic injury risk predictions were similar using the peak T12 acceleration and peak rib deflection methods outlined in [18] (19% versus 15% chance of AIS3+ injury). It has been suggested that lower spine accelerations may not be a good predictor of thoracic injury, but instead provide a good indication of overall loading to the thorax [18]. Interestingly, when the PMHS were evaluated for thoracic injury risk based on both T12 acceleration and peak half-lateral rib deflection, T12 acceleration was a better predictor of AIS3+ injury for every PMHS test (Table IV). On average from the five PMHS tests, T12 acceleration predicted a 68% chance of AIS3+ injuries while peak deflection only predicted 9%. All five PMHS tests resulted in AIS3 injury [21]. Although the SID-IIs demonstrated excellent biofidelity (BRS score <1) of T12 kinematics (Table II), Fig. 4 shows that the peak resultant acceleration of the ATD falls near the lower boundary of the corridor, peaking at approximately 10 gs less than the average PMHS peak resultant T12 acceleration. Additionally, the SID-IIs thoracic risk curves for the 5th percentile female were normalized to an age of 56 years based on a NASS-CDS analysis from 1993 to 2001 of the most frequently injured small females in side impacts [18]. These findings suggest the development of age-dependent injury risk curves specifically for side-impact loading scenarios where combined loading is present, which could more accurately represent the risk to this vulnerable population.

Limitations

This study is not without limitations. As with many PMHS tests, the sample size used to create the kinematic corridors was limited to five tests. Variability in both kinematic response and injury tolerance has been attributed to human variation in age, anthropometry and skeletal material properties. Although the inclusion criteria of the PMHS for this test targeted 5th percentile females, the data were not further normalised. Also of note, the study investigating PMHS response under combined loading targeted subjects that met the clinical standard for osteopenia based on areal bone mineral density (aBMD) to investigate a more vulnerable population. However, recent studies exploring the relationships between aBMD and injury outcomes have not shown strong correlations [35]. Combined loading in this study was achieved by using the ASIS to represent door intrusion. Differences in HyGE sled initiation resulted in differences in the performance of the individual ASIS cylinders, which may also contribute to differences seen in PMHS and ATD response. As discussed further in Bolte et al., the most critical intrusion cylinders were those loading the upper thorax and the pelvis (Figs. A1-A4, cylinders 1 and 3) [21].

At the time of publication, the WorldSID-05F is not a regulated ATD and therefore its injury prediction capabilities were not evaluated. However, the spinal kinematics of the WorldSID were good (BRS score<1), showing promise for the applications of this ATD in a combined loading scenario, though further investigation into the underprediction of thoracic deflection is required. Though efforts were taken in replicating initial seating positions, differences in ATD vs. PMHS positioning may contribute to differences in loading between the ATDs compared to the PMHS.

V. CONCLUSIONS

Despite similarities in kinematics between the ATDs and PMHS, both the internal instrumentation in the ATDs and the external chestband deflection data showed differences in thoracic response as compared to the small, elderly PMHS, suggesting a difference in overall thoracic stiffness between the ATDs and PMHS. Thoracic injuries occurring because of combined loading may not be accurately predicted by conventional injury metrics given that a majority of ATDs have been built for single-axis loading. Results from this study also suggest that current injury metrics might not be appropriate for defining injury risk curves for small, elderly female occupants.

VI. ACKNOWLEDGEMENTS

We are grateful to the anatomical donors whose selfless gifts made this research possible. We would also like to thank all of the students, faculty, and staff of the Injury Biomechanics Research Center at The Ohio State University for their considerable support.

VII. REFERENCES

[1] National Highway Traffic Safety Administration (NHTSA) (2022). Older 1019 population: 2020 data, traffic safety facts. 2022. Available at: https:// 1020 crashstats.nhtsa.dot.gov/Api/Public/ViewPublication/813341. Accessed 1 November, 2022.

[2] Noh, E. Y., Atwood, J. R. E., Lee, E., Craig, M. J. (2022) Female crash fatality risk relative to males for similar physical impacts. *National Highway Traffic Safety Administration,* 2022, Report No. DOT HS 813 358.

[3] Forman, J., Poplin, G. S., et al. (2019) Automobile injury trends in the contemporary fleet: Belted occupants in frontal collisions. *Traffic Injury Prevention*, **20**(6): pp.607–612. doi:10.1080/15389588.2019.1630825

[4] Bose, D., Segui-Gomez, M., Crandall, J. R. (2011) Vulnerability of female drivers involved in motor vehicle crashes: an analysis of US population at risk. *American Journal of Public Health*, **101**(12): pp.2368–2373.

[5] Sunnevång, C., Rosén, E., Boström, O., Lechelt, U. (2010) Thoracic injury risk as a function of crash severity in carto-car side impact tests with WorldSID compared to real-life crashes. *Annals of Advances in Automotive Medicine,* **54**: pp.159–168.

[6] Klinich, K. D., Bowman, P., Flannagan, C. A. C., Rupp, J. D. (2016) Injury patterns in motor-vehicle crashes in the United States: 1998-2014. Ann Arbor, MI: University of Michigan Transportation Research Institute. Report No. UMTRI-2016-16.

[7] Ramachandra, R., Kashikar, T., Bolte IV, J. H. (2017) Injury patterns of elderly occupants involved in side crashes. *Proceedings of IRCOBI Conference*, 2017, Antwerp, Belgium.

[8] Kong, J. S., Kim, O. H., *et al.* (2018) Analysis of injury mechanism of the 1005 elderly and non-elderly groups in minor motor vehicle accidents. *Traffic Injury Prevention*, **19**(sup2): pp.S151–S153. doi: 10.1080/15389588.2018. 1007 1532210.

[9] Viano, D. C. (1989) Biomechanical responses and injuries in blunt lateral impact. *Proceedings of 33rd Stapp Car Crash Journal,* 1989, 892432.

[10] Rhule, H., Suntay, B., *et al*. (2011) Response of PMHS to high- and low-speed oblique and lateral pneumatic ram impacts. *Stapp Car Crash Journal*, **55**.

[11] Shaw, J., Herriott, R., McFadden, J., Donnelly, B., Bolte, J. H. (2006) Oblique and lateral impact response of the PMHS thorax. *Stapp Car Crash Journal*, **50**: pp.147–167.

[12] Baudrit, P., Petitjean, A., Potier, P., Trosseille, X., Vallencien, G. (2014) Comparison of the thorax dynamic responses of small female and midsize male post mortem human subjects in side and forward oblique impact tests. *Stapp Car Crash Journal,* **58**: pp.103–121.

[13] Trosseille, X., Baudrit, P., *et al*. (2009) The effect of angle on the chest injury outcome in side loading. *Stapp Car Crash Journal,* **53**: pp.403–419.

[14] Cavanaugh, J., Walilko, T., *et al*. (1990) Biomechanical response and injury tolerance of the thorax in twelve sled side impacts. *SAE Technical Paper (SAE)*, 1990, Paper No. 902307.

[15] Kallieris, D., Mattern, R., Schmidt, G., Eppinger, R. H. (1981) Quantification of side impact responses and injuries. *Proceedings of 20th Stapp Car Crash Conference,* 1981, Paper No. 811009.

[16] Pintar, F. A., Yoganandan, N., *et al*. (1997) Chestband analysis of human tolerance to side impact. *Proceedings of Stapp Car Crash Conference,* **41**: Paper No. 973320.

[17] Riley, P. O., Arregui-Dalmases, C., *et al*. (2012) Kinematics of the unrestrained vehicle occupants in side-impact crashes. *Traffic Injury Prevention*, **13**(2): pp.163–171.

[18] Kuppa, S. (2006) Injury Criteria for Side Impact Dummies. U.S. Department of Transportation. Docket (NHTSA-2015-0119-0011).

[19] Yoganandan, N., Pintar, F., *et al*. (2007) Biomechanics of side impact: Injury criteria, aging occupants, and airbag technology. *Journal of Biomechanics*, **40**(2): pp.227–243.

[20] Sugaya, H., Takahashi, Y., *et al*. (2019) Development of a human FE model for elderly female occupants in side crashes. *Proceedings of 26th International Technical Conference on Enhanced Safety of Vehicles (ESV)*, 2019, Eindhoven, Netherlands.

[21] Bolte, IV J. H., Fibbi, C., *et al*. (2022) Analysis of injury mechanism and thoracic response of elderly, small female PMHS in near-side impact scenarios. *Traffic Injury Prevention.* In press.
[22] Federal Register (2007) Federal motor vehicle safety standards; Occupant protection in interior impact; Side impact protection; Side impact phase-in reporting requirements; Final Rule. 49 CFR 571 72(175): 51908-51973.
[23] Federal Register (2008) Consumer information; New car assessment program; Final Decision Notice. 49 CFR 571, **73**(134): pp.40016–40050.
[24] Insurance Institute for Highway Safety (2022) Side impact crashworthiness evaluation 2.0; Crash test protocol; Version II. Arlington, VA: Insurance Institute for Highway Safety.
[25] SAE J211 (2014) Instrumentation for impact test—Part 1: electronic 1027 instrumentation. SAE paper no. J211/1_201403. SAE International.
[26] Pintar, F., Humm, J., Yoganandan, N., Martin, P. (2009) Test program to 1025 define oblique chest loading in side impact. 21st ESV Conference. Paper No. 09–0057.
[27] Boxboro Systems (2017) RibEye Multi-Point Deflection Measurement System Software User Manual (Version 5.3).
[28] Hagedorn, A., Stammen, J., et al. (2022) Biofidelity Evaluation of THOR-50M in Rear-Facing Seating Configurations Using an Updated Biofidelity Ranking System. *SAE International Journal of Transportation Safety*, **10**(2): pp.291–375. doi: 10.4271/09-10-02-0013.
[29] Kuppa, S. (2006) Injury Criteria for Side Impact Dummies. U.S. Department of Transportation. Docket (NHTSA-2015-0119-0011).
[30] Irwin, A. L., Crawford, G., Gorman, D., Wang, S., Mertz, H. J. (2016) Thoracic injury risk curves for rib deflections of the SID-IIs Build Level D. *Stapp Car Crash Journal*, 60: pp.545-580.
[31] Ikeda, M. and Mae, H. (2017) Comparison of thorax responses between WorldSID-5th and SID-IIs in lateral and oblique impacts. 25th ESV Conference. Paper No. 17-0364.
[32] Yoganandan, N., Humm, J., *et al*. (2012) 1042 Thoraco-abdominal deflection responses of post mortem human surrogates in side impacts. *Stapp Car Crash Journal*, **56**: pp.49–64. doi: 10. 4271/2012-22-0002.
[33] Insurance Institute for Highway Safety (2022) Side impact crashworthiness evaluation 2.0; Rating guidelines; Version III. Arlington, VA: Insurance Institute for Highway Safety.
[34] Haverfield, Z., Hunter, R. L., Loftis, K. L., Agnew, A. M. (2022) Skeletal site and method-dependent variability of bone mineral density in injury biomechanics research. IRCOBI. IRC-22-49: pp.332–360.

VIII. APPENDIX

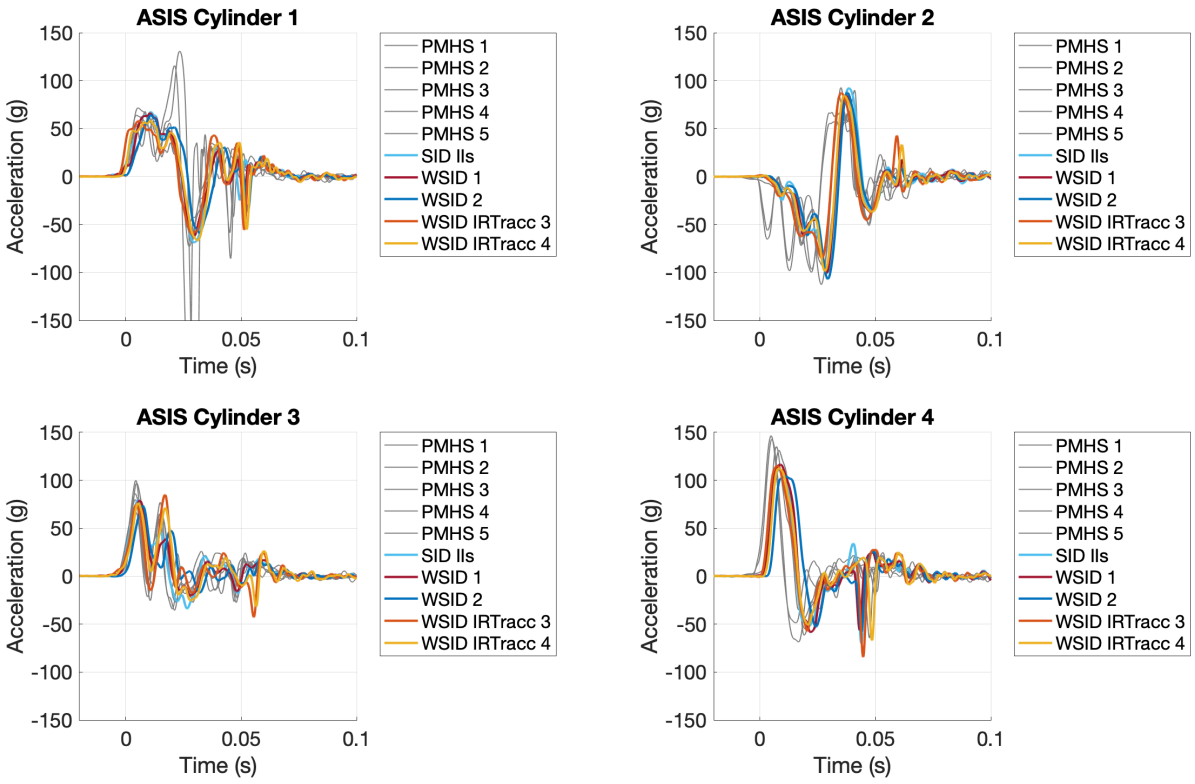

Fig. A1. ASIS cylinder acceleration repeatability.

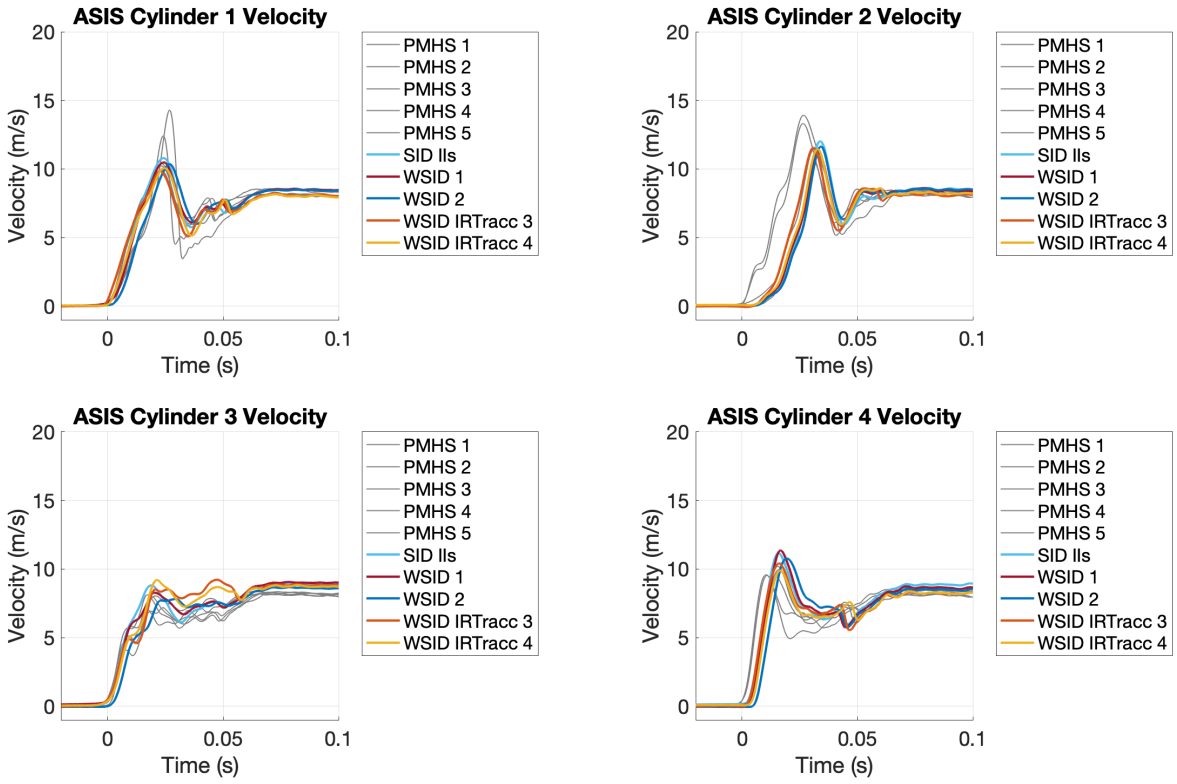

Fig. A2. ASIS cylinder velocity repeatability .

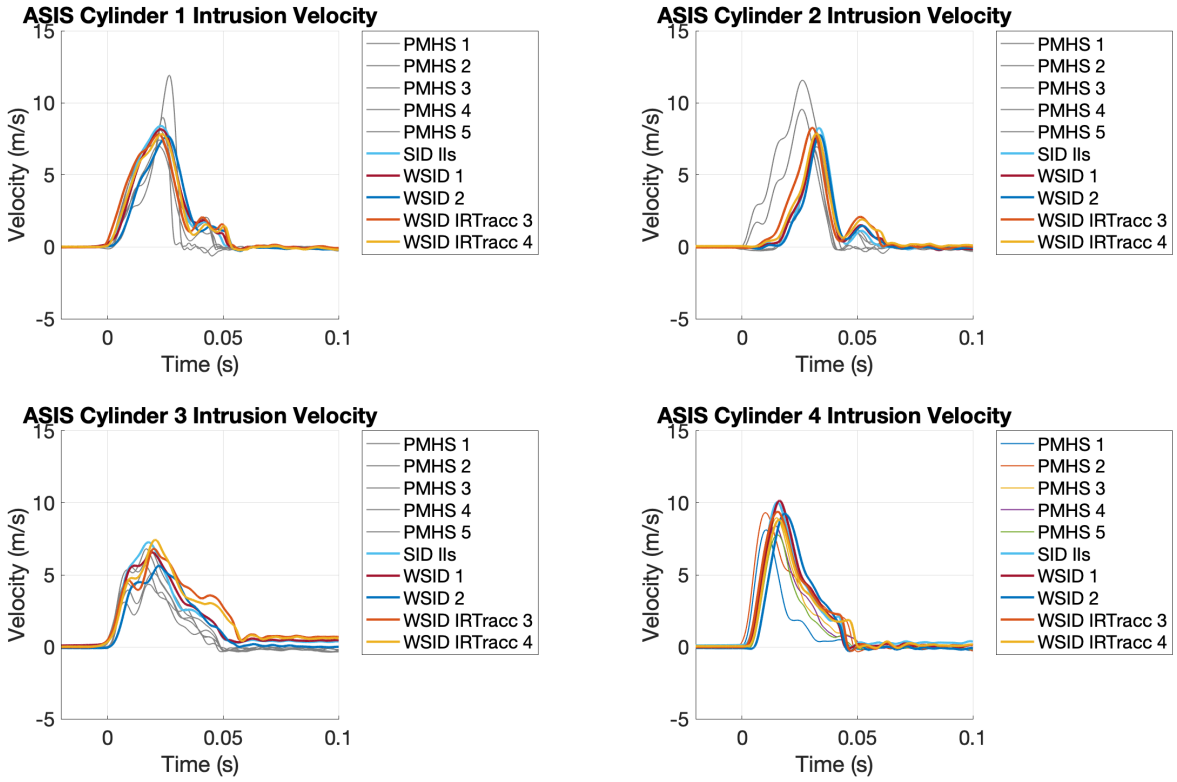

Fig. A4. ASIS cylinder intrusion velocity repeatability.

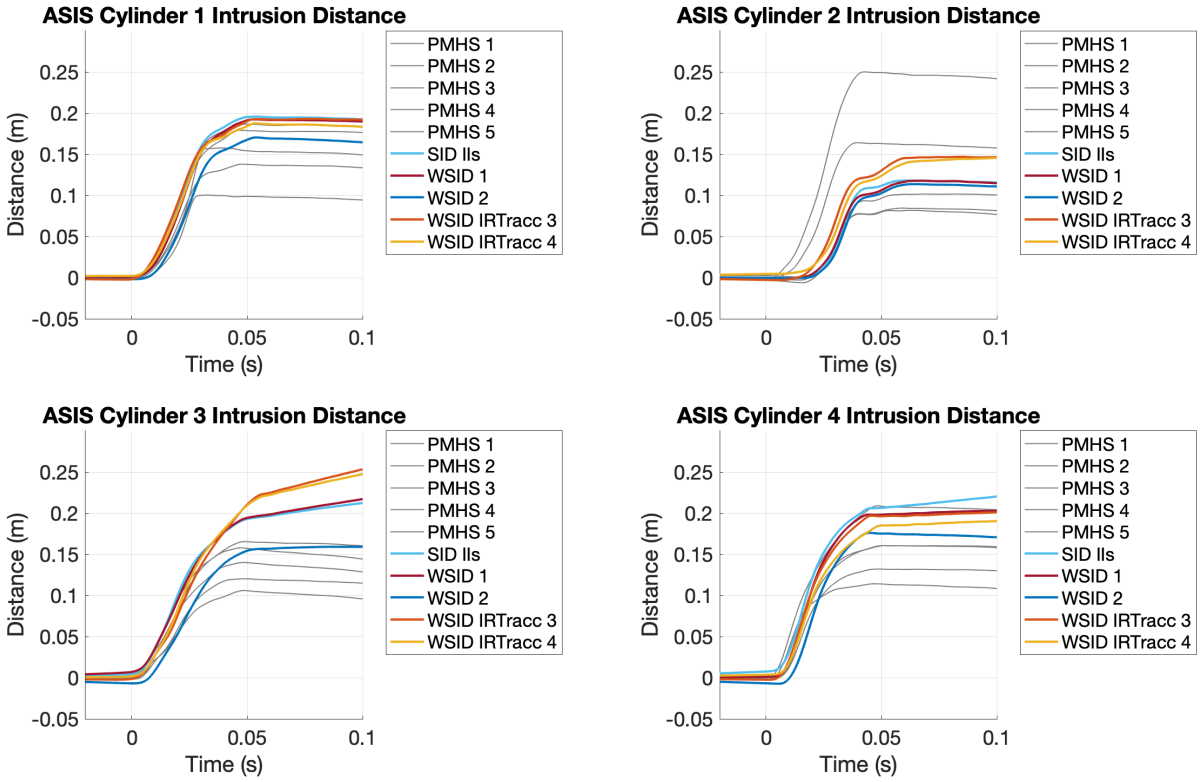

Fig. A4. ASIS cylinder intrusion distance repeatability.

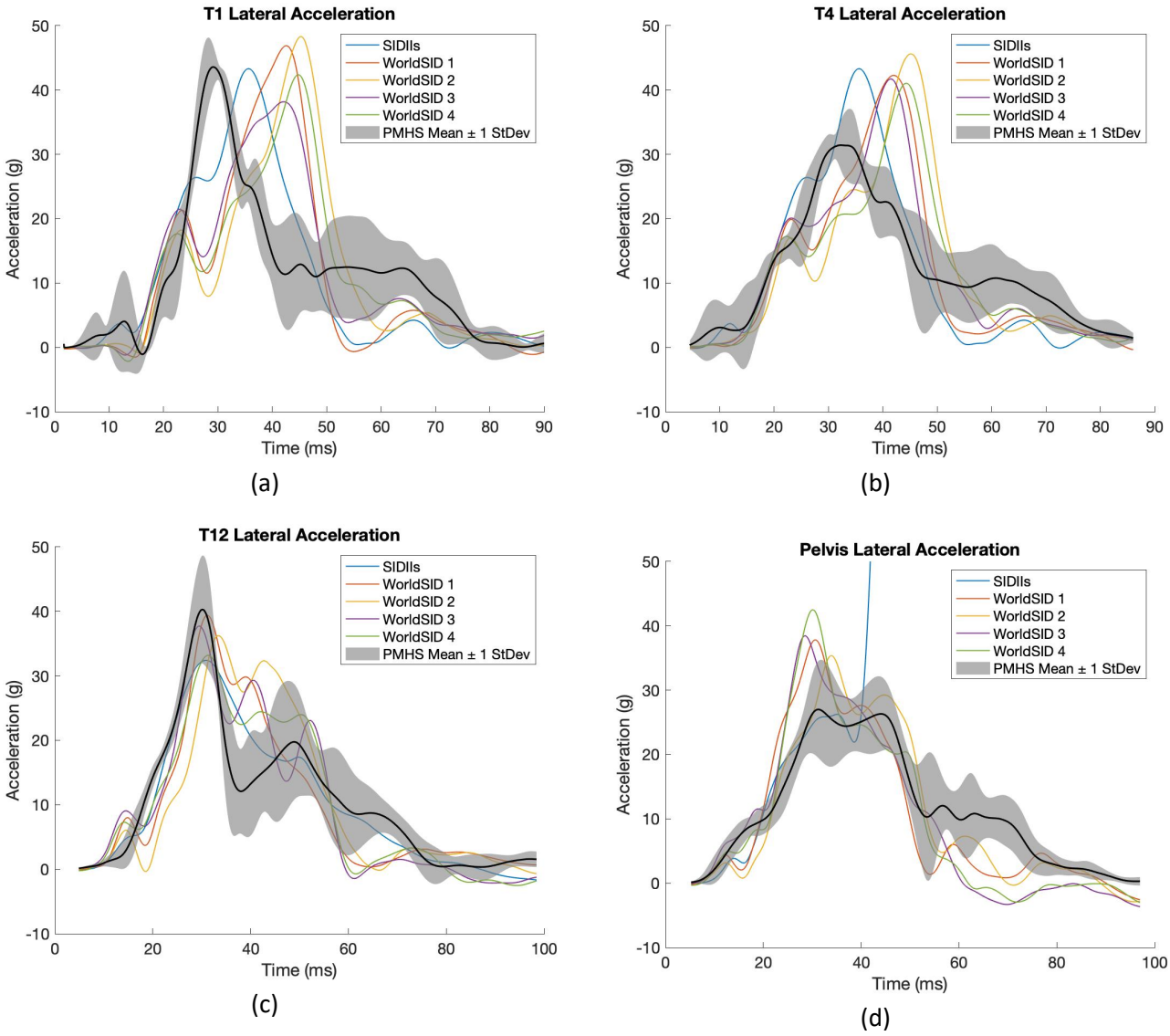

Fig. A5. ATD comparison to PMHS response corridors of lateral acceleration for (a) T1, (b) T4, (c) T12 and (d) pelvis.

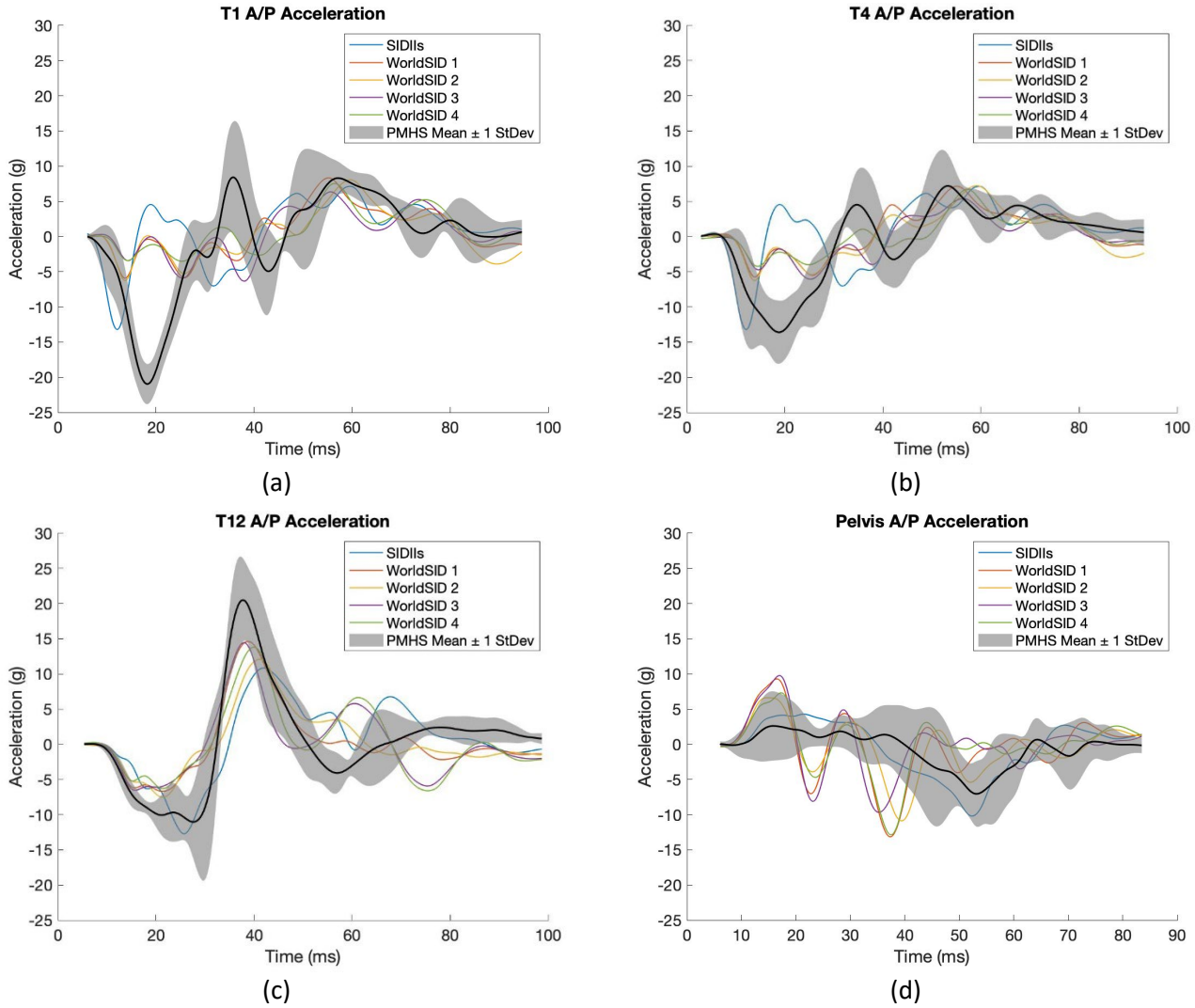

Fig. A6. ATD comparison to PMHS response corridors of A/P acceleration for (a) T1, (b) T4, (c) T12 and (d) pelvis.

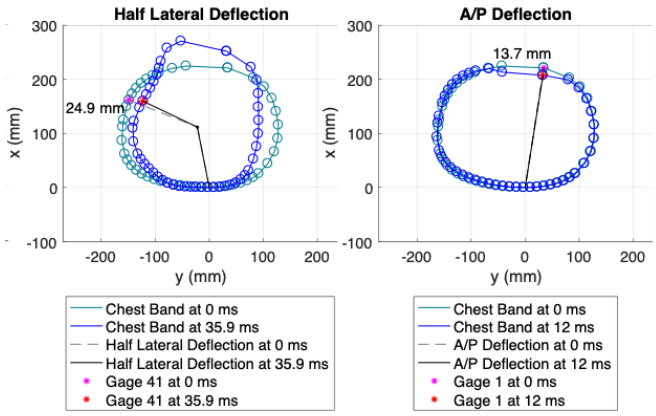

Fig. A7. Chestband contours from an axilla mounted chestband on the SID-IIs shown at maximum (a) half-lateral deflection and (b) A/P deflection.

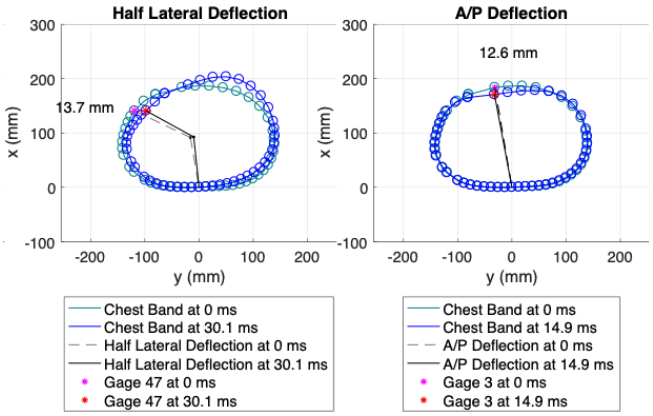

Fig. A8. Chestband contours from an axilla mounted chestband on the WorldSID-05F (test 1) shown at maximum (a) half-lateral deflection and (b) A/P deflection.

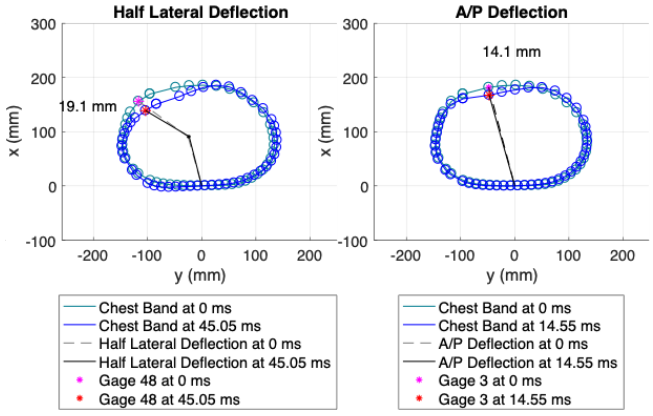

Fig. A9. Chestband contours from an axilla mounted chestband on the WorldSID-05F (test 2) shown at maximum (a) half-lateral deflection and (b) A/P deflection.

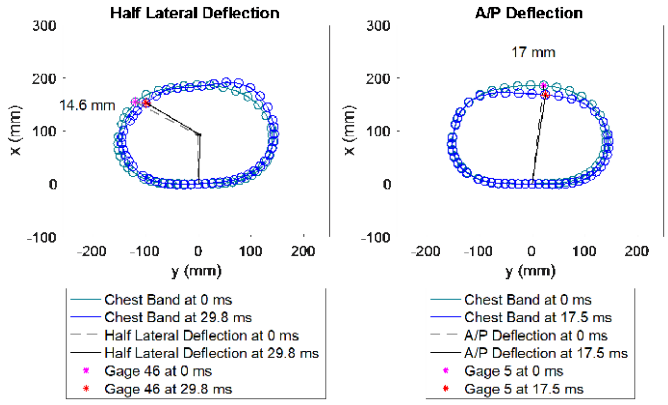

Fig. A10. Chestband contours from an axilla mounted chestband on the WorldSID-05F (test 3) shown at maximum (a) half-lateral deflection and (b) A/P deflection.

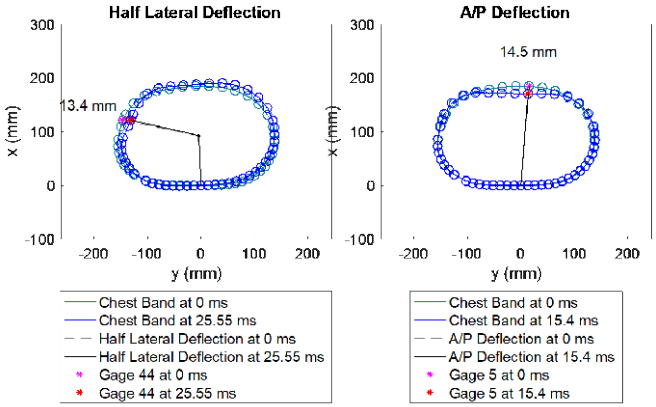

Fig. A11. Chestband contours from an axilla mounted chestband on the WorldSID-05F (test 4) shown at maximum (a) half-lateral deflection and (b) A/P deflection.

TABLE A-I

SUMMARY OF T1 ACCELERATION BRS SCORES BY ATD AND DIRECTION

	T1 A/P	T1 Lateral	T1 Resultant
SID-IIs	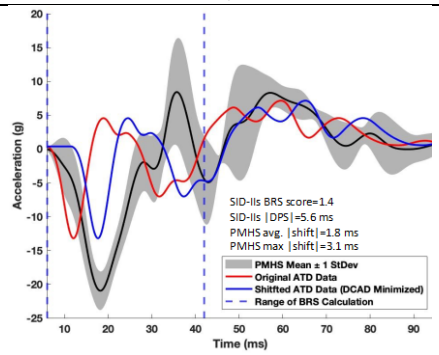	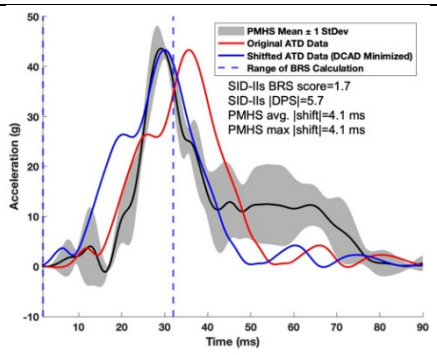	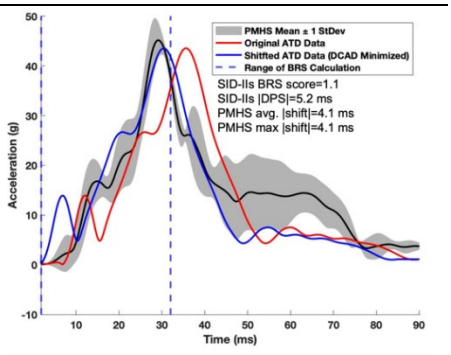
WorldSID test 1	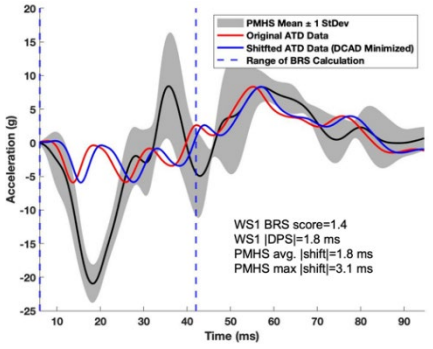	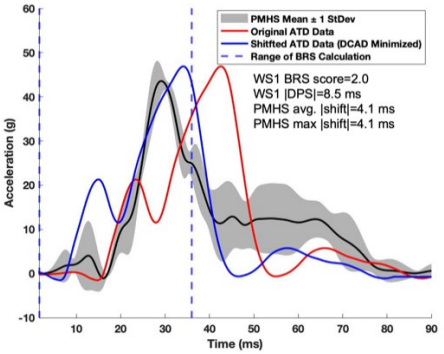	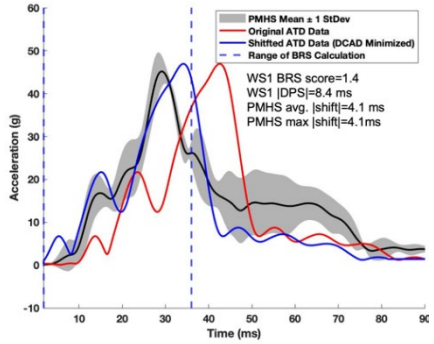
WorldSID test 2	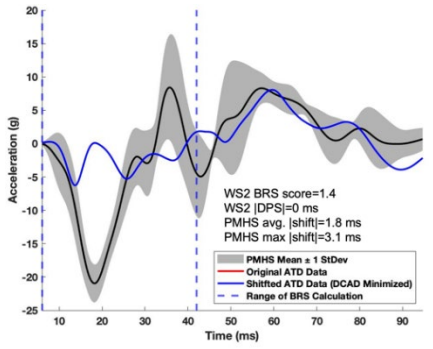	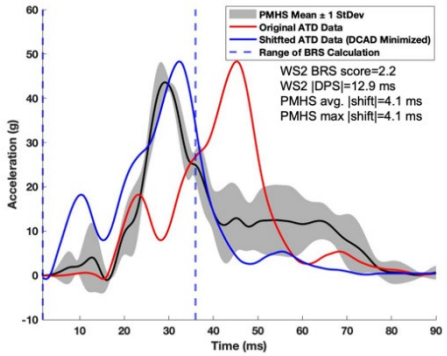	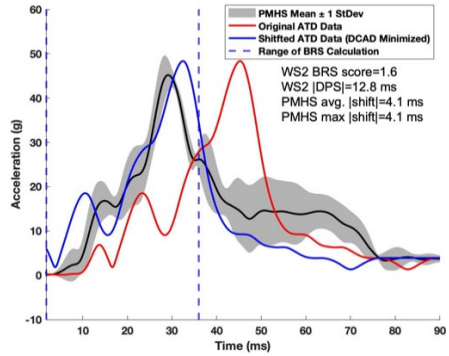
WorldSID test 3	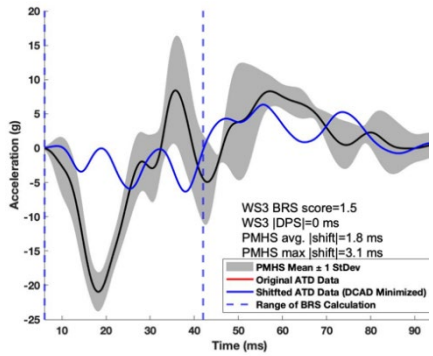	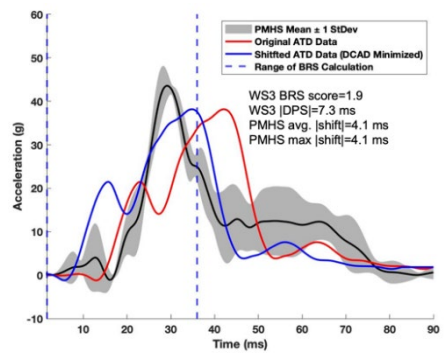	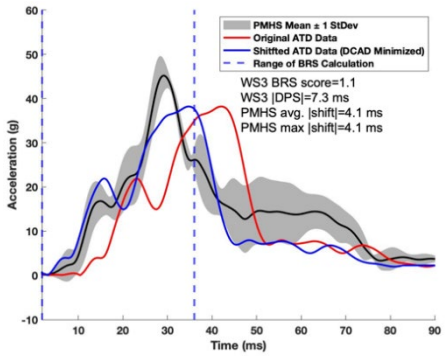
WorldSID test 4	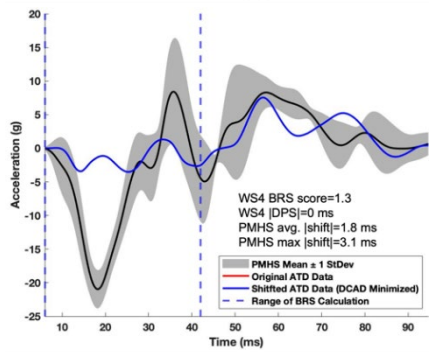	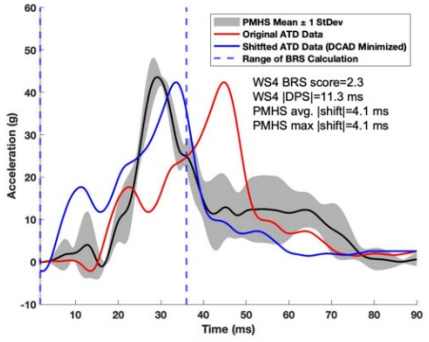	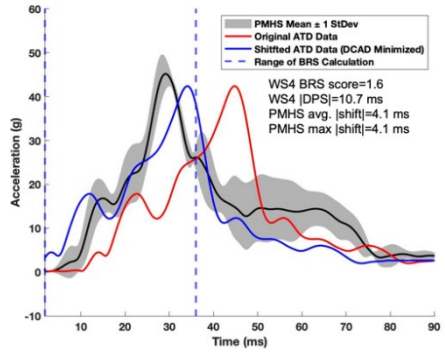

TABLE A-II

SUMMARY OF T4 ACCELERATION BRS SCORES BY ATD AND DIRECTION

	T4 A/P	T4 Lateral	T4 Resultant
SID-IIs	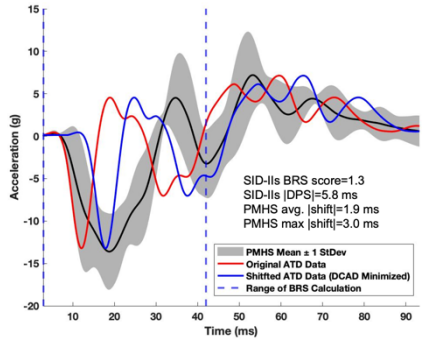	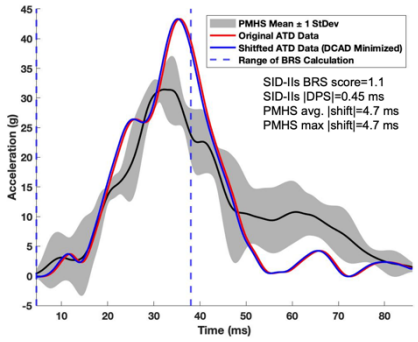	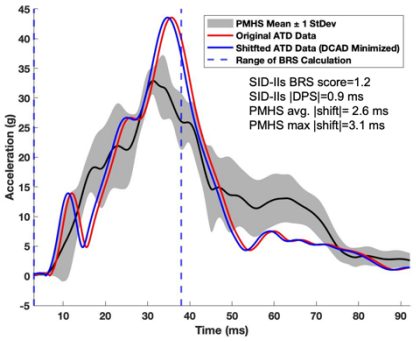
WorldSID test 1	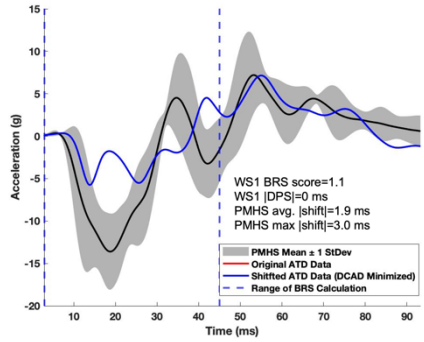	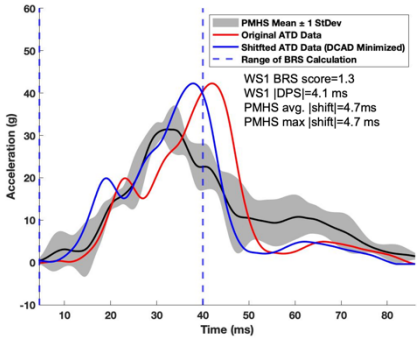	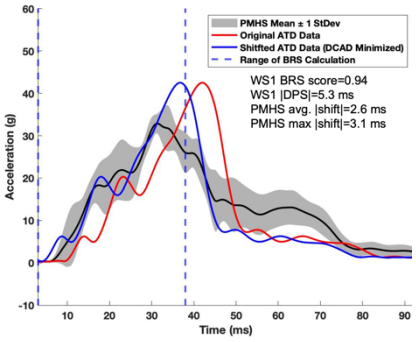
WorldSID test 2	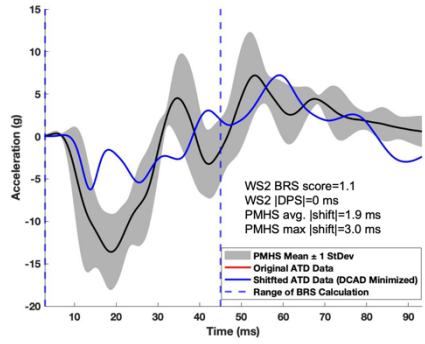	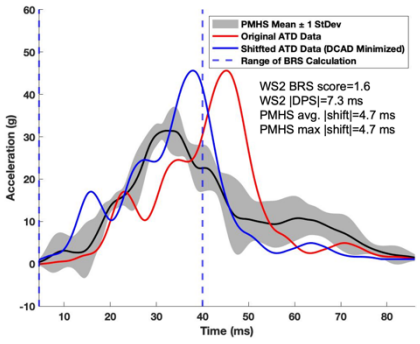	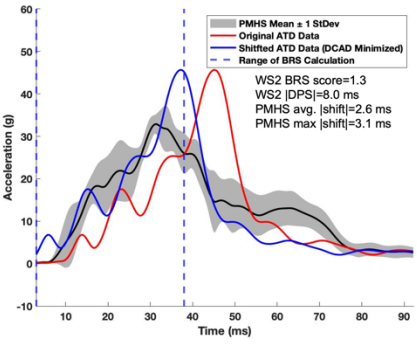
WorldSID test 3	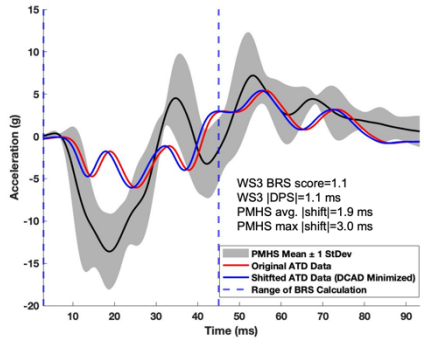	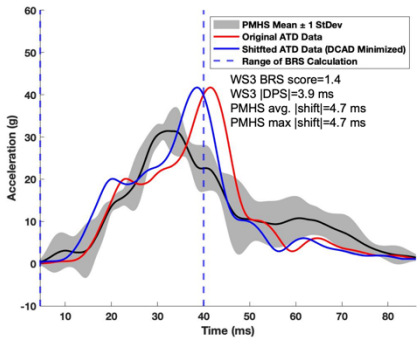	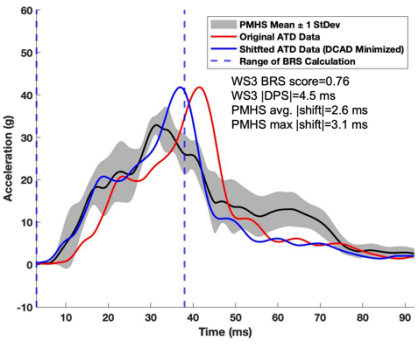
WorldSID test 4	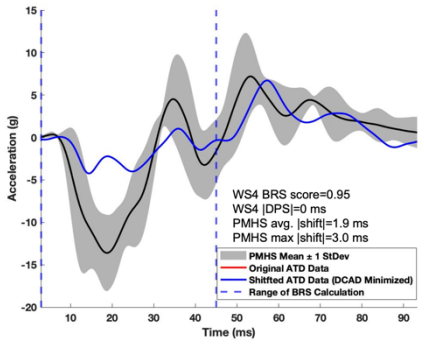	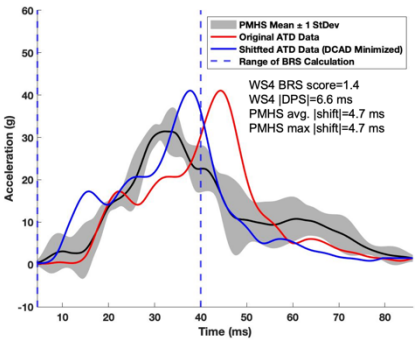	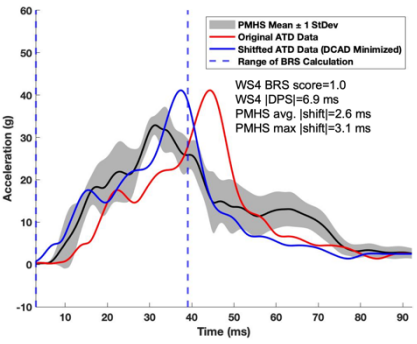

TABLE A-III

SUMMARY OF T12 ACCELERATION BRS SCORES BY ATD AND DIRECTION

	T12 A/P	T12 Lateral	T12 Resultant
SID-IIs	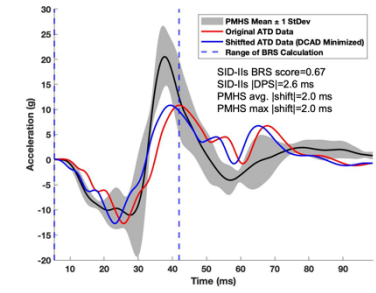	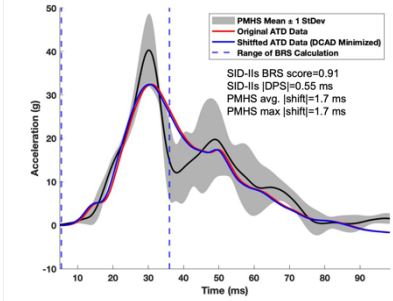	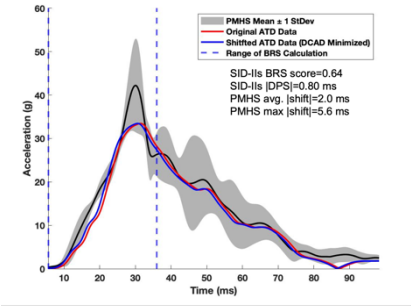
WorldSID test 1	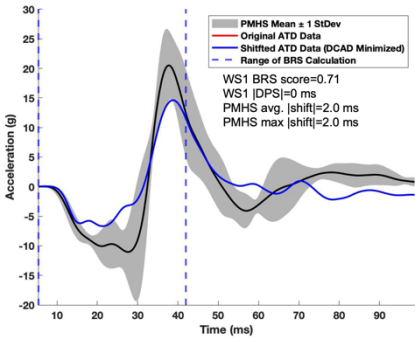	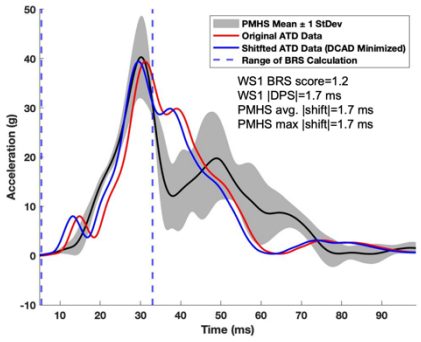	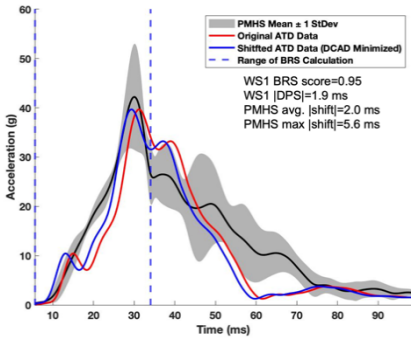
WorldSID test 2	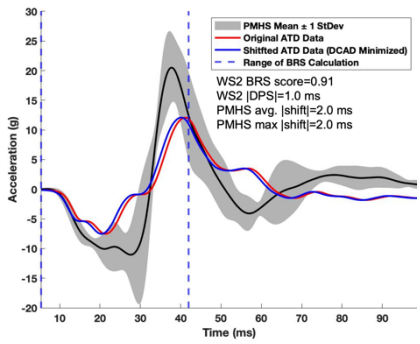	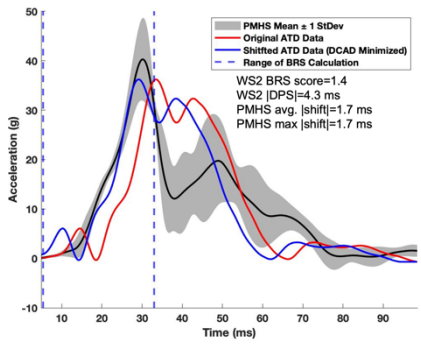	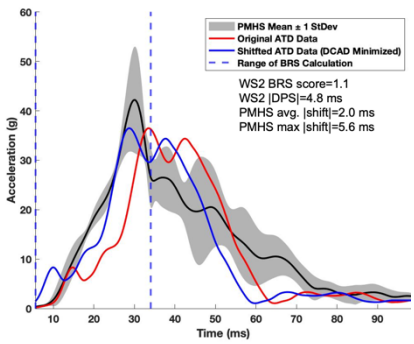
WorldSID test 3	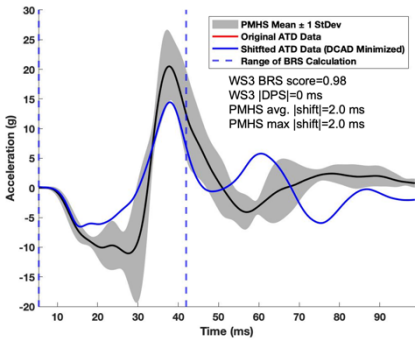	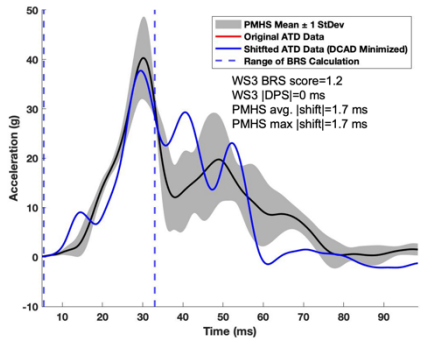	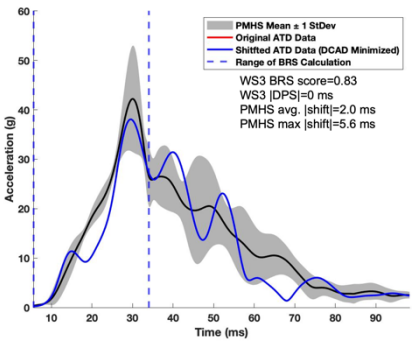
WorldSID test 4	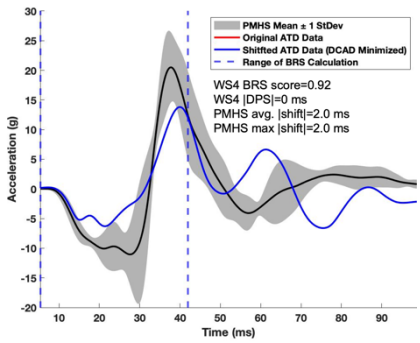	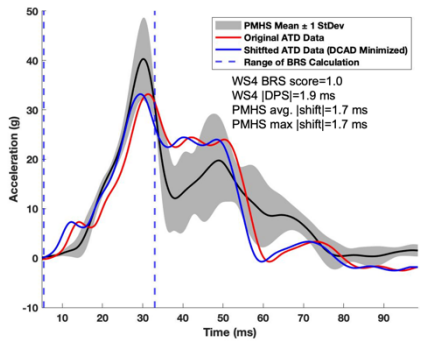	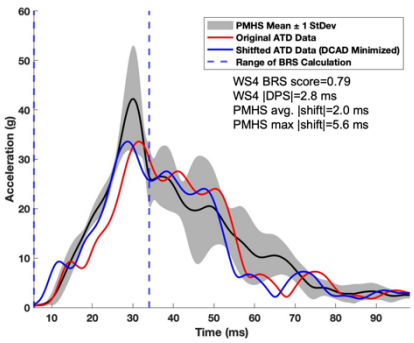

TABLE A-IV
SUMMARY OF PELVIS ACCELERATION BRS SCORES BY ATD AND DIRECTION

	Pelvis A/P	Pelvis Lateral	Pelvis Resultant
SID-IIs	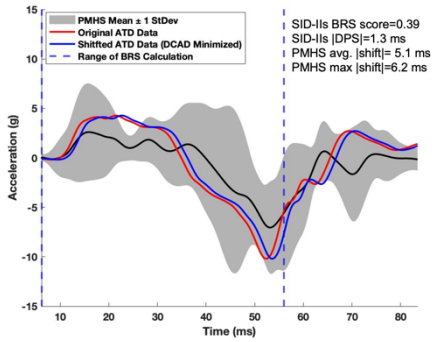	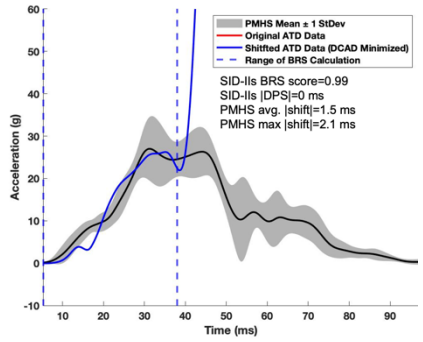	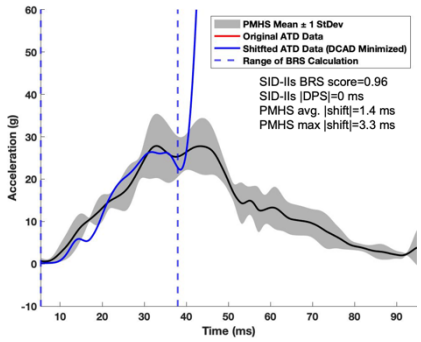
WorldSID test 1	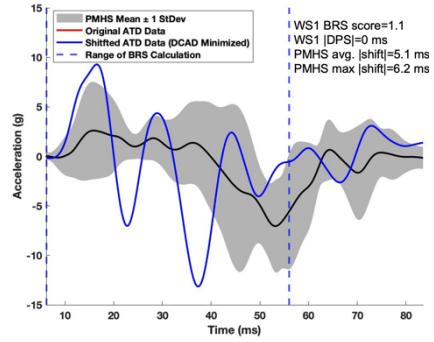	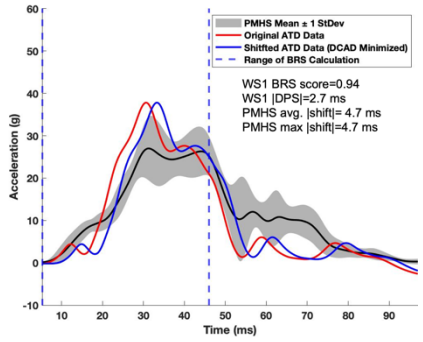	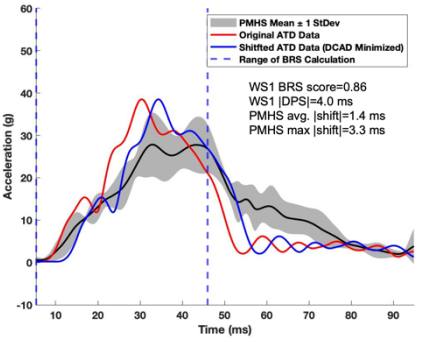
WorldSID test 2	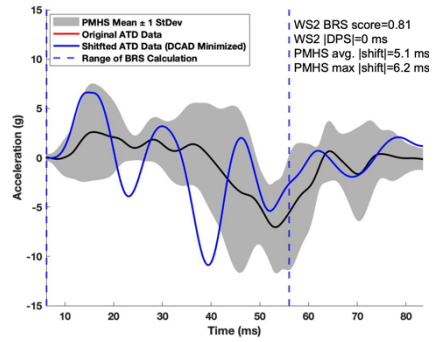	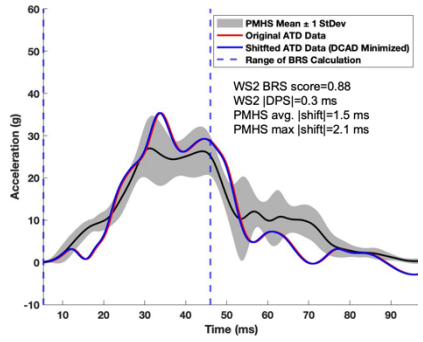	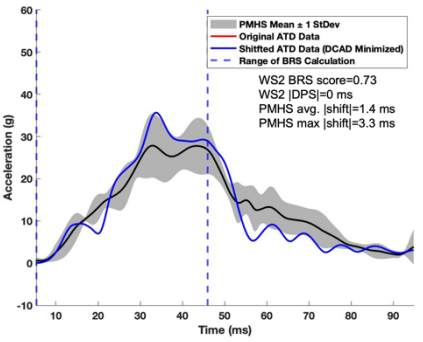
WorldSID test 3	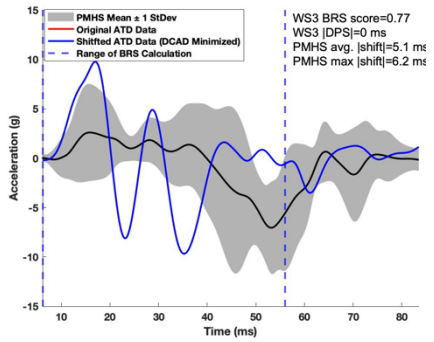	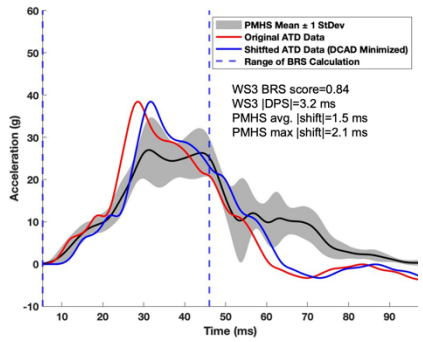	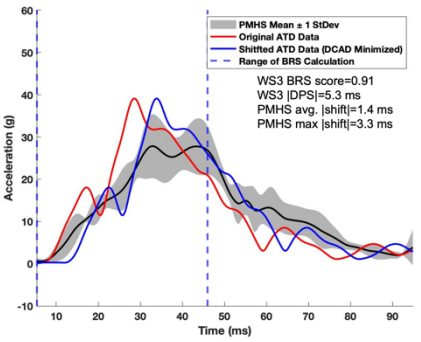
WorldSID test 4